Drones and Other Technologies to Assist in Disaster Relief Efforts

Research Final Report from the University of Tennessee Knoxville | Shuai Li, Amirsalar Moslehy, Da Hu, Mengjun Wang, Nicholas Wierschem, Khalid Alshibli, and Baoshan Huang | May 31, 2022

Sponsored by Tennessee Department of Transportation Long Range Planning Research Office & Federal Highway Administration

DISCLAIMER

This research was funded through the State Planning and Research (SPR) Program by the Tennessee Department of Transportation and the Federal Highway Administration under ***RES 2021-05: Drones and Other Technologies to Assist in Disaster Relief Efforts.***

This document is disseminated under the sponsorship of the Tennessee Department of Transportation and the United States Department of Transportation in the interest of information exchange. The State of Tennessee and the United States Government assume no liability of its contents or use thereof.

The contents of this report reflect the views of the author(s) who are solely responsible for the facts and accuracy of the material presented. The contents do not necessarily reflect the official views of the Tennessee Department of Transportation or the United States Department of Transportation.

Technical Report Documentation Page

1. Report No. RES2021-05	2. Government Accession No.	3. Recipient's Catalog No.
4. Title and Subtitle *Drones and Other Technologies to Assist in Disaster Relief Efforts*		5. Report Date May 2022 6. Performing Organization Code
7. Author(s) Shuai Li, Amirsalar Moslehy, Da Hu, Mengjun Wang, Nicholas Wierschem, Khalid Alshibli, Baoshan Huang		8. Performing Organization Report No.
9. Performing Organization Name and Address Department of Civil and Environmental Engineering The University of Tennessee, Knoxville 325 John D. Tickle Engineering Building 851 Neyland Drive, Knoxville, TN, 37996		10. Work Unit No. (TRAIS) 11. Contract or Grant No. RES 2021-05
12. Sponsoring Agency Name and Address Tennessee Department of Transportation 505 Deaderick Street, Suite 900 Nashville, TN 37243		13. Type of Report and Period Covered Final report September 2020 – May 2022 14. Sponsoring Agency Code
15. Supplementary Notes Conducted in cooperation with the U.S. Department of Transportation, Federal Highway Administration.		

16. Abstract

Tennessee faces many threats from natural disasters such as storm, flooding, landslide, and earthquake, which damage civil infrastructure and cause major service interruptions. The application of emerging technologies such as drones, sensing technologies, machine learning methods, and optimization techniques in disaster preparedness, response, and recovery have gained substantial attention. This research first reviewed the current practice and system configurations for using drones and other emerging technologies in disaster relief efforts, providing useful insights for TDOT to understand the uses of these technologies. A generalizable framework based on 3D reconstruction, deep learning, and optimization was proposed for processing drone-acquired data and drone mission planning, which can be applied in various disaster scenarios. Thereafter, the use cases as well as general workflows for using drone systems and software tools in different types of disaster scenarios were studied, including post-disaster infrastructure systems surveys, landslide investigation, and flooding assessment. Pilot tests were also conducted to validate the proposed methods, use cases, and workflows, confirming the feasibility and potential of using drones and associated technologies in disaster relief efforts, and therefore providing TDOT useful information for potential implementation.

17. Key Words		18. Distribution Statement	
Drones, Disaster Relief, Use Cases, Workflow		No restriction. This document is available to the public from the sponsoring agency at the website http://www.tn.gov/.	
19. Security Classif. (of this report) Unclassified	20. Security Classif. (of this page) Unclassified	21. No. of Pages 45	22. Price

Acknowledgment

This project partially supported the following presentations and publications.

Hu, D., Li, S., Du, J., and Cai, J. (2022). Automating Building Damage Reconnaissance to Optimize Drone Mission Planning for Disaster Response. ASCE Journal of Computing in Civil Engineering, Under Review.

Hu, D., Chen, J.,and Li, S. (2022). Reconstructing unseen spaces in collapsed structures for search and rescue via deep learning based radargram inversion. Automation in Construction, 140, 104380.

Hu, D., Chen, L., Du, J., Cai J., and Li, S. (2022). Seeing through Disaster Rubble in 3D with Ground-Penetrating Radar and Interactive Augmented Reality for Urban Search and Rescue, ASCE Journal of Computing in Civil Engineering. 10.1061/(ASCE)CP.1943-5487.0001038.

Moslehy, A., Alshibli, K. A., Li, S. (2021) "Unmanned Aerial Vehicles (UAVs): Opportunities & Challenges" American Society of Highway Engineers (ASHE)-Middle Tennessee, 9/22/2021.

Moslehy, A., Alshibli, K. A., Li, S. (2021) "Unmanned Aerial Vehicles (UAVs): Opportunities & Challenges" 2021 Tennessee Engineering Conference, Nashville, TN, Sept. 12-14, 2021.

List of Acronyms

Abbreviation	Definition
TDOT	Tennessee Department of Transportation
LiDAR	Light detection and ranging
SFM	Structure from motion
CNN	convolutional neural network
GPR	Ground penetrating radar
LDV	laser Doppler vibrometer
TIR	Thermal infrared
GIS	geographic information system
RTK	real-time kinematic positioning
GCPs	ground control points
DTM	digital terrain model
CAD	Computer Aided Drawing
RG	region growing
YOLO	You Only Look Once
CSPNet	Cross Stage Partial Networks
SPPF	Spatial Pyramid Pooling Fast
VRPP	Vehicle Routing Problem with Profits
TS	Tabu search
ISBDA	Instance Segmentation in Building Damage Assessment
SGD	Stochastic Gradient Descent
GA	Genetic Algorithm
AP	Average precision
UAV	unmanned aerial vehicle
A.G.L.	above the ground level

Executive Summary

The purpose of this project is to expedite the use of emerging technologies such as drones at the Tennessee Department of Transportation (TDOT) for disaster preparedness, response, mitigation, and recovery. Tennessee faces many threats from natural disasters such as tornadoes, flooding, landslides, and earthquakes, which damage civil infrastructure and cause major service interruptions. TDOT plays critical roles in preparing for, mitigating, responding to, and recovering from disasters. The use of advanced and emerging technologies such as drones, sensing technologies, machine learning methods, and optimization techniques could significantly expedite disaster relief efforts. However, before deploying these technologies to assist disaster relief efforts, TDOT needs to address two important questions. First, what technologies are available for TDOT to assist disaster relief efforts? Different types of disasters, different site conditions, and different tasks of emergency management require the use of different technologies. TDOT needs an in-depth understanding of the available technologies and their applications in different disaster scenarios. Second, how these technologies can be best used by TDOT? To use the technologies in an effective and efficient manner, information must be collected to develop tools, use cases, and workflows for potential implementation in the state of Tennessee. Therefore, addressing the two questions is urgent and critical for TDOT to use the advanced and emerging technologies in disaster reliefs.

To address the critical needs, this research reviewed the current practice and system configurations for using drones and other emerging technologies in disaster relief efforts, providing useful insights for TDOT to understand the uses of these technologies. In addition, a generalizable framework based on 3D reconstruction, deep learning, and optimization was proposed for processing drone-acquired data and drone mission planning, which can be applied in various disaster scenarios. The framework can be adapted based on the needs from TDOT for potential implementation. This research also investigated the use cases as well as general workflows for using drone systems and software tools in different types of disaster scenarios, including post-disaster infrastructure systems surveys, landslide investigation, and flooding assessment. Pilot tests were also conducted to validate the proposed methods, use cases, and workflows, confirming the feasibility and potential of using drones and associated technologies in disaster relief efforts, and therefore providing TDOT useful information for potential implementation.

Key Findings

The key findings of this research were summarized below.

- This research led to a critical review of the hardware systems of drones and sensing technologies for application in different disaster relief efforts, sharpening TDOT’s understanding about the capability and applicability of the emerging technologies.
- This research led to a generalizable method for using drones and artificial intelligence-enabled software/data processing tools, providing TDOT an implementable framework to collect, process, and analyze critical data before, during, and after disasters for disaster preparedness, response, and recovery. The framework was tested and validated using the data collected during the Tennessee tornado disasters, offering TDOT implementation

insights for using the framework. 3D reconstruction can achieve due accuracy with drone-collected images, and the 3D model can be used in various analysis for disaster relief efforts. Deep learning methods were also found effective in processing drone-collected images to extract disaster-relevant information, but good performance requires substantial training data which may be difficult to acquire.

- This research produced use cases and workflow for using drones in different types of disaster scenarios for potential implementation in Tennessee. The implementation of these advanced technologies will help address several concerns that TDOT is facing with, including post-disaster infrastructure surveys, landslides and floods, therefore, could help TDOT to improve the efficiency and effectiveness of disaster relief efforts.
- The potential and feasibility for using drones in disaster relief efforts such as post-disaster infrastructure survey and structure assessment and landslide investigation were demonstrated via field experiments, confirming the promise of drones to assist disaster relief efforts.

Key Recommendations

- With appropriate system configurations, drones can be used in various scenarios for disaster relief efforts to expedite the task implementation, improve data collection, and reduce survey and assessment time, as well as improve safety during disaster relief efforts. It should also be noted that different types of drones should be operated for different types of disaster scenarios, considering the constraints and limits of the drone systems, the requirement of disaster relief tasks, and the nature and environmental conditions of the disasters.
- Commercial software and tools are available to control drones and process drone-collected data for common applications such as 3D reconstruction. 3D reconstruction of disaster scene or structures of interest could provide useful models for subsequent analysis such as damage assessment and slope failure analysis. In addition, deep learning techniques can be applied to process drone-collected images for extracting disaster-relevant information with due accuracy. To achieve better performance, large amounts of training data are needed for more robust performance in disaster relief efforts.
- The uses of drones in disaster relief efforts such as post-disaster infrastructure survey and assessment, landslide investigation, and flooding assessment are recommended. The workflows differ in different types of disasters and for different stages such as disaster preparedness, mitigation, response, and recovery.
- Practitioners need to carefully evaluate the workflow and use cases for practical applications, particularly in the challenging environments after disasters that involves many uncertainties.

Table of Contents

List of Tables

List of Figures

Chapter 1 Introduction

1.1 Research Problem

Tennessee faces many threats from natural disasters such as storms, flooding, landslides, and earthquakes, which damage civil infrastructure and cause major service interruptions. Facing the increase in number and severity of natural disasters, there is a critical need for the TDOT to enhance their technical capability in preparing for, responding to, mitigating the consequences of, and recovering from disasters. Recently, the use of advanced technologies such as drones and sensing technologies in disaster preparedness, response, and recovery have gained substantial attention. However, before deploying these technologies to assist disaster relief efforts, TDOT needs to address two important questions. First, what technologies are available for TDOT to assist disaster relief efforts? Different types of disasters, different site conditions, and different tasks of emergency management require the use of different technologies. TDOT needs an in-depth understanding of the available technologies and their applications in different disaster scenarios. Second, how these technologies can be best used by TDOT? To use the technologies in an effective and efficient manner, information must be collected to develop tools, use cases, and workflows for potential implementation in the state of Tennessee. Therefore, addressing the two questions is urgent and critical for TDOT to use the advanced and emerging technologies in disaster reliefs.

1.2 Research Objectives

The overarching goal of this research is to expedite the use of emerging technologies such as drones at TDOT for disaster preparedness, response, mitigation, and recovery. Three research objectives were pursued in this project.

- **Objective 1: Identify and study hardware systems that can be used for disaster relief.** The research team identified a few hardware systems that can be used in disaster relief and reviewed the appropriate configurations of the hardware systems for disaster relief applications.
- **Objective 2: Identify and study software systems that can be used for disaster relief.** The research team identified and reviewed software systems that can be used in disaster relief, and developed a generalizable framework based on 3D reconstruction, deep learning, and optimization for using drones in disaster relief.
- **Objective 3: Develop use cases and workflows for potential implementation.** The research team assessed the applicability and efficacy of using drones in different disaster scenarios, and documented use cases and general workflows of using the technologies for potential TDOT implementation.

1.3 Work Scope and Methods

The scope of work and methodological approaches to address TDOT's critical needs are elaborated as follows.

- **TDOT's need to identify and study hardware systems for disaster relief.** An in-depth understanding of the hardware systems and constraints for usage in disaster areas could help TDOT safely, effectively, and efficiently operate the systems and avoid failures and accidents. The research team assessed the suitability of operating different hardware systems, identified the appropriate system configurations, and documented the data collection requirements in different types of disasters.

- **TDOT's need to identify and study software systems for disaster relief.** Under time pressure and workforce shortage during emergency response, TDOT needs appropriate software systems in place to automate the processing of large amounts of data collected by the hardware systems. The research team reviewed different software/data analysis tools and developed a generalized framework for using drones and artificial intelligence (AI) based methods for processing data to assist disaster relief efforts.
- **TDOT's need to develop use cases and workflow for potential implementation.** TDOT plays important roles in preparing for, responding to, mitigating the consequences of, and recovering from disasters. The research team assessed the applicability of drone technologies in disaster relief efforts in Tennessee and developed use cases and workflows of applying the emerging technologies in different types of disaster relief scenarios.

1.4 Outcomes and Research Significance

This research led to the following outcomes and may yield significant benefits to TDOT.

- This research led to a critical review of the hardware systems of drones and sensing technologies for application in different disaster relief efforts, sharpening TDOT's understanding about the capability and applicability of the emerging technologies.
- This research led to a generalizable method for using drones and AI-enabled software/data processing tools, providing TDOT an implementable framework to collect, process, and analyze critical data before, during, and after disasters for disaster preparedness, response, and recovery. The framework was tested and validated using the data collected during the Tennessee Tornado disasters, offering TDOT implementation insights for using the framework.
- This research produced use cases and workflow for using drones in different types of disasters scenarios for potential implementation in Tennessee. The implementation of these advanced technologies will help address several concerns that TDOT is facing with, including post-disaster infrastructure surveys, landslides and floods, therefore, could help TDOT to improve the efficiency and effectiveness of disaster relief efforts.

Chapter 2 Literature Review

In Chapter 2, the application of drones and other emerging technologies in different disaster scenarios are reviewed, including post-disaster infrastructure and structure survey and assessment, landslide investigation, and flooding assessment. The hardware configuration and software uses were investigated to provide insights for potential TDOT implementation.

2.1 Post-Disaster Infrastructure Survey and Assessment

Structures including buildings, bridges, roads, and other civil infrastructure systems can be damaged after disasters. It is very critical for TDOT to identify the defects and assess the damages of civil infrastructure systems and buildings after disasters to better plan for disaster relief efforts. One of the key applications is the assessment of bridges and other structures. The drone-assisted assessment of structures has been studied and implemented as related to routine structural inspections and as a part of a post-disaster response [1,2]. The application of drones to structural assessment introduces some new challenges. Unlike other drone applications that primarily require top-down sensing or imaging, typically from a significant height, the assessment of structures could require sensing or imaging of objects below the drone, to the side (due to the vertical nature of structures), and above (for example the underside of a bridge). Furthermore, due to the nature of structural assessment, sensing or imaging may be required closer to the target (the structure in this case) than for other types of assessment [3]. Typically, structural assessments examine structural members and connections for signs of damage or deterioration. Items of note include cracking, tearing, bulging, bearing movement, spalling, section loss, rust, water stains, paint conditions, bolt conditions, and other defects or abnormalities [4]. Visual imaging from still images or videos are the main tool for structural assessment using drones and can be used to observe most of the above signs of damage or deterioration. For some of these items, including cracks, it is important that this imaging is high-quality and high-resolution [5]. Furthermore, relatively close flight of the drone to the structure is needed to capture sufficient imaging [3]. In addition to visual imaging, there is interest and has been research in equipping drones with other types of sensor systems including light detection and ranging (LiDAR) or laser imaging, hyperspectral imaging, thermal imaging, radiation detectors, humidity sensors, and temperature sensors [6,7].

Drones incorporate different levels of technology and automation for application in infrastructure survey and assessment. While some drones are remotely piloted by humans in real-time, some drones operate more autonomously with pre-planned missions and are supervised by an operator. Flight planning software is required to enable this autonomous operation. Commercial flight planning software for drones include Mission Planner, DJI Ground Station Pro, Pix4d Capture and Drone deploy [6]. Typical commercial flight planning software utilizes a graphical interface in which a mission is laid out. These mission components include waypoints, tasks for the drone at the waypoints, and tasks for the drone in between waypoints. The drone can also be commanded with this software to switch in and out of manual mode as desired. One mission type that is of particular importance to the application of drones for structural assessment is one supporting 3D model reconstruction; however, many flight planning software do not have an effective option available for automated capturing of the necessary imagery at low altitude for structural 3D reconstruction [8]. In addition to selecting waypoints for drones, flight planning software can be used to determine how the drone travels between the configured waypoints. Options include not specifying the trajectory, specifying the trajectory, and enabling obstacle avoidance along a trajectory [6]. If a trajectory is not specified, the trajectory can be optimized by the software for speed or drone endurance.

3D models reconstructed from data collected from drones are used to identify many signs of structural damage or deterioration. The construction of these 3D models can be done with many different techniques. One of the most important 3D model reconstruction methods uses the photogrammetry technique structure-from-motion (SFM) [6]. This technique can be used to create 3D models of entire structures or models of particular areas of interest, such as a connection. The SFM technique works using a large number of images of the target from perspectives all around the target. Furthermore, commercial software is available, such as Agisoft Metashape, that automates this process and requires only the image files to run. Compared to a 3D model produced with LIDAR, it was found in this case that the SFM 3D model of the bridge had a higher noise level than the LIDAR derived model, but the SFM model was denser and more complete [9]. 3D models of structures can be used in multiple techniques to detect damage from disasters and other sources. This includes techniques that exploit machine learning, including convolutional neural network (CNN)-based structural damage detection and classification. Cracks can be identified in structural members using images and videos from drone in real-time or after a flight by a human inspector and without the need for additional processing and software [10].

Underwater infrastructure systems, for example dams, levees, bridge piers, and harbor piers, must be inspected regularly as part of disaster prevention, preparation, and recovery [11–14]. Considering the significant number of underwater bridge piers in Tennessee and previous bridge failures caused by bridge pier scours in Tennessee such as the 1989 Hatchie River US-51 bridge failure [15–17], bridge pier inspections are critical. Underwater drones can provide a safer and more accurate inspection for underwater infrastructure systems when compared to divers' inspection [12,14,18]. Bridge pier inspection to detect potential scours normally requires divers to spend a long time under the water to inspect the bridge piers, which involves a tremendous amount of risk and danger [19–22]. DeVault [19] designed an underwater drone with an embedded video camera to capture videos of bridge piers for scour inspection. Ueda et al. [14] introduced a bridge pier inspection device using an underwater drone and concluded that the developed system is capable of imaging cracks found on underwater structures. Pauly & Skrocki [21] examined the possibility of employing underwater drones for bridge pier inspection for the Michigan Department of Transportation. They compared the underwater drone inspection results with previously performed divers' inspection and found that scour inspection conducted using the underwater drone can be as accurate as divers' inspection. Using sonar sensors installed on the underwater drone could also increase the accuracy of the scour mapping results. Park et al. [23] developed a 2 MHz sonar sensor that can obtain higher-resolution sonar scans when compared with the existing 1 MHz sonar sensors in bridge inspections. To create a map of the scanned bridge pier or other underwater infrastructure the sonar scans should be processed. The majority of the commercial sonar systems come with proprietary software that can collect the reflected sonar signals and create a 3D cloud point of the surveyed area [21]. The collected 3D cloud point can then be imported to computer-aided drawing (CAD) software for viewing, editing, or further analyses. Some underwater drone systems use a combination of visual cameras in addition to a sonar sensor to create a better understanding of the mapping region.

In this case, a software system capable of using both the images acquired by the cameras and the sonar signals in creating the map of the scanned underwater infrastructure should be used.

Subsurface infrastructure systems such as sewers, water, oil, gas, and steam pipelines are society's lifelines and can be disrupted by various disasters including earthquakes and floods [24,25]. Failures of these infrastructure systems could also cause disasters due to potential explosions or contaminations [26–29]. Excavating the ground to inspect subsurface infrastructure systems as part of disaster prevention, preparation, and recovery is extremely tedious, costly, and most often not capable of identifying all the subsurface infrastructure failures [30,31]. Recent advancements in drones and sensors can be leveraged to conduct non-destructive inspections on subsurface infrastructures [32,33]. For instance, drones equipped with thermal cameras or ground penetrating radars (GPR) can be used to assist the mapping and inspection of subsurface infrastructure systems to reduce associated costs [33,34]. Colorado et al. [35] designed a drone equipped with GPR for detecting buried objects made of at least 30% metal. This drone system was capable of detecting objects larger than 0.08 m in diameter buried about 0.2 m in the ground. Zhang et al. [36] investigated the effects of GPR antenna height and angle on the detection of nonmetallic buried objects. The results showed that scanning the soil at 0.7 m above the ground and an antenna angle of 60° significantly increases the signal strength and therefore the quality of the mapping for identifying nonmetallic buried objects. Garcia-Fernandez et al. [32,37] examined mounting a GPR on a DJI M600 Pro RTK [38] drone to detect buried objects. The developed drone was fully capable of detecting both metallic and nonmetallic objects buried at a depth of about 0.2 m. Sugimoto et al. [39] proposed using acoustic irradiation-induced vibration to detect buried objects. The proposed setup is composed of a commercial sound source that can be mounted on drones and a laser Doppler vibrometer (LDV) (such as PSV-500 Scanning Vibrometer [40]). This setup was more successful in identifying buried objects in wet soil compared to GPR-based buried object detection that performs better in dry soils. Thermal infrared (TIR) cameras are useful tools for inspecting subsurface infrastructure carrying fluids with a heat gradient compared to the soil medium [33]. Shakmak & Al-Habaibeh [41] examined the possibility of detecting water leakage in buried pipelines using high-resolution and low-resolution TIR cameras. Kavi & Halabe [31] investigated the feasibility of detecting buried pipelines carrying hot fluids using a TIR camera.

2.1 Drone-Assisted Landslide Investigation

Landslides are devastating disasters that slowly develop in multiple stages and can have various causes [42]. Every year hundreds of landslides occur in Tennessee, some of which were initiated many years ago by small earthquakes (especially in western Tennessee) and develop slowly while some are caused by excessive rainfalls [43–45]. Drones with advanced integrated sensors can be used to identify and monitor areas prone to landslides as part of disaster preparation and prevention measures, and map landslides post-failure for the purpose of disaster recovery [46–48]. Identifying areas with landslide potentials can be conducted by obtaining high-quality aerial images of the studied region, creating a topographic map of the area using photogrammetry, and analyzing the topographic map using geographic information system (GIS) techniques [47,49,50]. Aerial images captured using drones equipped with real-time kinematic positioning (RTK) GPS systems often yield a much more accurate topographic map [51]. Additionally, using ground control points (GCPs) can further improve the accuracy of the topographic maps created using aerial images [49]. To Identify the slopes with potential for landslides, first, a topographic map or a digital terrain model (DTM) of each slope needs to be obtained. The images captured using drones need to be processed using photogrammetry techniques to create a topographic map or a DTM of the slope. In the photogrammetry process, SFM techniques are used to create a 3D model of the surveyed area and then generate a DTM model of the slope. The DTM models created in the previous step then can be imported into a GIS platform to perform further analyses. The required software systems, therefore, are a photogrammetry software solution capable of creating a DTM model of the slope and a GIS platform for handling the created DTM model and the assessment factors. Commercial photogrammetry software such as Pix4Dmapper [52], Agisoft [53], and DJI Terra [54] are some examples of the current accessible software that are capable of performing the required processes. Slope saturation by rainwater is one of the main landslide causes [49]. Drones capable of carrying a TIR camera, and heavier payloads such as ground penetrating radar sensors can be used to monitor the moisture content of a slope, which can provide a timely warning prior to the failure [55,56]. Monitoring the stability of the slopes with the potential for landslides by estimating their moisture content is somewhat new and requires developing non-commercial frameworks [48,55,56].

Mapping a landslide post-failure topography is the first step in disaster recovery efforts to examine the stability of the site post-failure, create a map of the affected region for designing the proper stabilization plans, estimate the volume of the materials needed for reconstruction, and determine the causes of the landslide [46,57–59]. A drone system equipped with RTK modules and coupled with GCP GPS receivers (similar to the hardware needed for identifying areas prone to landslides) is proven to produce an accurate 3D map of the landslide [46,59]. Although using optical images can result in highly accurate topographic maps, LiDAR scanners can map an area with more vegetation coverage more accurately due to the fact that the light pulses produced by a LiDAR scanner can penetrate through openings of the vegetation and reflect from the ground yielding a better representation of the actual terrain [58]. Mapping a landslide post-failure similar to identifying the slopes with potential for landslides requires creating a DTM model of the slope and then analyzing the model in GIS software or CAD software [46,57,59].

2.3 Drone-Assisted Flooding Survey and Assessment

Floods are one of the most common natural disasters which account for about a third of total losses caused by natural disasters [60–62]. The majority of the streams in the Cumberland and Tennessee river basins experience a major flood with a recurrence interval of 1 to 50 years [63,64]. Flood risk assessments, identifying flooded areas during floods, and post-flood damage evaluations are essential parts of disaster preparation, response, and recovery efforts. However, traditional techniques for performing the assessments are relatively slow, may be low in resolution, and in certain cases simply are not practical [61,65,66]. For example, post-flood damage evaluations immediately after the flood cannot be performed using traditional surveying equipment. drones can offer robust flood risk assessments, identify the flooded areas during flood response efforts, and evaluate post-flood damages [65,67,68].

Creating a topographic map of watersheds and basins is the initial step in flood risk assessments. Coveney & Roberts [67] proposed using drone-based photogrammetry data to create river flood-risk models. The drone employed in this study was a SenseFly Swinglet CAM [69] fixed-wing aircraft. In addition, Coveney & Roberts [67] implemented various numbers of GCP sets with the drone photogrammetry data to discover the optimal number of GCPs needed for producing reliable spatial measurements. Annis et al. [60] utilized a similar approach as Coveney & Roberts [67] by using drones coupled with GCPs for assessing flood risk. Moreover, in addition to comparing drone-generated flood-risk assessment maps with available public flood-risk assessment maps, they compared the drone-generated maps with LiDAR-generated maps. The drone-generated flood-risk assessment maps were found to be significantly more accurate than the available public flood-risk management maps and as accurate as the maps created by LiDAR scanning. Optical photos acquired using drones can produce highly accurate flood-risk assessment maps where the stream depth is shallow and the vegetation is not dense; however, they cannot be used where the stream is deep and the vegetation is heavy [61]. LiDAR scanning by drones is a viable solution for relatively deep streams and areas covered by thick vegetation [61].

Drone optical photos and data can also be employed for detecting flooded areas for direct disaster response activities [62,65]. For this purpose, the affected area must be surveyed, and the flooded areas must be identified from the survey. Popescu et al. [62] developed an algorithm that can identify the flood extents based on segmenting images acquired by drones into flooded pixels and non-flooded pixels. Although this technique can yield fairly accurate results in wide-open areas, it falls short in detecting flood extents underneath vegetation canopies [65]. Optical granulometry is a technique for identifying grain size distribution based on images that can be employed post floods to detect changes in flood depositions, embankments, and rip-raps [68]. Optical granulometry requires capturing high-quality images of the affected area, where the individual soils grains are visible. Langhammer et al. [68] used drone-based optical images to compare the flood depositions pre and post-floods. Langhammer et al. [68] concluded that drone-based optical granulometry is capable of detecting the changes in flood depositions pre and post-floods.

The software needed for creating flood-risk assessment maps from drone collected data can be divided into two categories. First, a photogrammetry solution should be used to create a DTM of the watershed. The quality of the flood-risk assessment maps that can be generated from the created DTM by the photogrammetry software is highly influenced by the accuracy of the elevations in the DTM model. Villanueva et al. [66] concluded the flood-risk assessment maps created using Agisoft PhotoScan [53] are significantly closer to the reference flood-risk assessment maps. Second, the generated DTM model can be imported into various hydraulic modeling or GIS software solutions (like ArcGIS [70]) to generate flood-risk assessment maps [60,66,67]. Detecting flooded areas during disaster response efforts requires image segmentation to identify the areas covered by water [62,65]. This process includes identifying the pixels representing water bodies, which can be performed by image processing software. However, as noted by Hashemi-Beni & Gebrehiwot [65] drone-based optical images might not be sufficient to detect water bodies underneath vegetation canopies. Hashemi-Beni & Gebrehiwot [65] developed a CNN coupled with a region growing (RG) method to detect the water bodies underneath thick vegetation covers. This coupled technique uses previously established flood detection surveys to train the CNN for detecting water bodies underneath vegetation that is not visible in the acquired optical images. Comparing the final output of the

CNN-RG method with the reference validation data, this technique is proven to be highly accurate for detecting flooded areas using drone acquired optical images.

Chapter 3 Methodology

In Chapter 3, first the hardware system and configurations that are suitable for disaster relief efforts are reviewed, which can be used for collecting data. In addition, considerations on setting up and operating different drone systems are discussed. Second, a software tools and a generalizable framework are proposed to process the drone-collected data to acquire situational awareness during disaster relief efforts. The data processing framework consists of steps for 3D reconstruction, object detection using deep learning-based techniques, and drone mission planning using optimization methods. The proposed framework can be customized and applied in various disaster scenarios.

3.1 Hardware System Configurations and Considerations

TABLE I summarizes the drone hardware systems used in recent disasters. TABLE II summarizes the sensor configurations for using drones in different types of disaster scenarios. The identified drone hardware, system configuration, and application scenarios could provide useful reference and insights for TDOT to select, test, and use drones and integrated sensing technologies for disaster relief efforts.

TABLE I
DRONES USED IN RECENT DISASTERS

Year	Disaster	UAS	Fixed-wing	Rotary	Search	Mapping	Structure inspection
2005	Hurricane Katrina	AeroVironment	✓	n/a	✓	✓	n/a
		Evolution	✓	n/a	✓	✓	n/a
		ISENSYS T-Rex	n/a	✓	✓	✓	n/a
		Silver Fox	✓	n/a	✓	✓	n/a
2005	Hurricane Wilma	ISENSYS T-Rex	n/a	✓	n/a	✓	✓
2007	Berkman Plaza 2 collapse	ISENSYS IP3	n/a	✓	n/a	n/a	✓
2010	Haiti Earthquake	Elbit Skylark	✓		n/a	✓	n/a
2011	Christchurch Earthquake	Parrot AR.Drone	n/a	✓	n/a	n/a	✓
2011	Tohoku Earthquake	Pelican	✓		n/a	n/a	✓
2011	Fukushima Nuclear Emergency	Honeywell T-Hawk	n/a	✓	n/a	✓	✓
2011	Evangelos Florakis Naval Base Exploration	AscTec Falcon	n/a	✓	n/a	✓	✓
		AscTec Hummingbird	n/a	✓	n/a	✓	✓
2011	Thailand Floods	FIBO UAV-1	✓	n/a	n/a	✓	n/a
		FIBO UAV Glider	✓	n/a	n/a	✓	n/a
		SIAM UAV	✓	n/a	n/a	✓	n/a
2012	Finale Emilia Earthquake	NIFTi 1	n/a	✓	n/a	n/a	✓
		NIFTi 2	n/a	✓	n/a	n/a	✓
2013	Lushan China Earthquake	HW18 (Ewatt HoverWings)	✓	✓	✓	✓	n/a
2013	Boulder Colorado Floods	Falcon Fixed	✓	n/a	n/a	✓	n/a
2014	SR530 Mudslides	DJI Phantom	n/a	✓	n/a	✓	n/a
		AirRobot 100	n/a	✓	n/a	✓	n/a
		PrecisionHawk	✓	n/a	n/a	✓	n/a
2015	Bennett Landfill SC	PrecisionHawk	✓	n/a	n/a	n/a	n/a
2017	Hurricane Harvey	DJI Phantom 4	n/a	✓	✓	n/a	✓
2017	Hurricane Irma	DJI Phantom 4 Pro	n/a	✓	n/a	✓	n/a
		Mavic Pro	n/a	✓	n/a	✓	n/a
2017	Mexico City Earthquake	DJI Phantom 4	n/a	✓	n/a	✓	n/a
2018	California Camp Fire	DJI Mavic 2 Enterprise	n/a	✓	n/a	✓	n/a
		DJI Phantom 4 Pro	n/a	✓	n/a	✓	n/a

TABLE II

SENSOR CONFIGURATIONS AND APPLICATIONS

Application	***Description***	***Example***	***Hardware***	***Raw data***	***Process outcome***
Monitoring, forecasting, and early warning	Create early warning system	Assess landslide evolution and provide early warnings [71]	RGB camera; GPS; IMU	RGB image	3D point cloud
		Monitor geohazards in reservoir region [72]	RGB camera; GPS; IMU	RGB image	Surface displacement
Standalone communication system	Re-establish the damaged or destroyed communication infrastructure	Provide Resilience in Wireless Sensor Networks [73]	ZigBee wireless module; Raspberry; Arduino; Antenna	Radio wave	Network
Mapping and reconnaissance	Disaster extent detection	Application of an algorithm to detect flood areas Automatically [74]	RGB camera; GPS; IMU	RGB image; RGB video	Flood extent
	Generate 3D model of disaster sites	Drone-based 3D model reconstruction visualization [75]	Stereo camera; GPS; IMU; AHRS	RGB image	3D model
		Use a low-cost LiDAR to reconstruct disaster environment [76]	INS; GNSS; LiDAR	Point cloud	3D point cloud
Damage assessment	Visual detection of damaged infrastructure	Detect and assess the damage of civil infrastructure [77]	RGB camera; thermal camera; GPS; IMU	RGB image; thermal image	Location of affected properties
	Resistance and resilience measures identification	Identification of residential properties with resistance Measures [78]	RGB camera GPS; IMU	RGB image	Orthoimage, DEM
Search and rescue	Identification of safe shelter points	Identify where to best place NGO camps and identify land that could be safer to relocate families	RGB camera GPS; IMU	RGB image; RGB video	Map with location of points
	Detection of stranded people	The use of UAS to locate stranded people even at night [79,80]	RGB camera; thermal camera; GPS; IMU	RGB image; RGB video; thermal image	Victim location
	Evacuation routes identification	Modeling of evacuation routes by using UAS as end devices of M2M architecture [81]	RGB camera	RGB image; RGB video	Map of evacuation route

There are some considerations for using drone systems during disaster relief efforts. Navigation by GPS positioning is common for drones that operate with a degree of autonomy. However, drones used for structural assessment may operate in close proximity to structures, including underneath bridges; thus, the loss or lack of GPS signal is a distinct possibility. Furthermore, the lack of GPS signal can prevent some drones from being able to even maintain a stable stationary position [10]. Drones must have alternate navigation systems to remain operational in GPS-denied environments or in the event of unexpected GPS loss. One option that has been investigated is the use of an ultrasonic beacons system [82]. This strategy requires pre-planning and some deployed resources as it uses stationary ultrasonic beacons at known points to determine the location of a drone with a mobile ultrasonic beacon. Alternatively, stability in a GPS-denied environment can be achieved with the addition to the drone of a stereovision system for position control and a sonar system for altitude control, both systems that require sensors only on the drone [10]. Another strategy is that in the event of GPS signal loss, the drone navigates based on an internal compass; however, if this strategy is to be relied upon, the drone's compass should be recalibrated prior to flight [5].

As still imaging or videos are two of the main tools used by drones for structural inspections and close-up detailed imaging is often required, lighting conditions for drone imaging is very important [77]; however, lighting conditions for structural assessment are not always ideal. For exterior inspections, lighting conditions will vary throughout the day due to the relative position of the sun. Furthermore, the structure itself will serve to block the sun as in the case of the shaded side of a structure or the underside of a bridge. Relatively open structural systems that only partially block the sun may result in lighting conditions that rapidly change and include glare. The capability of built-in or supplemental imaging systems to adjust to changes in lighting vary and must be considered when selecting a system [5]. To compensate for low lighting conditions, drones can be configured with attached lighting systems [5]. While these lighting systems can improve imaging quality, their weight and energy demands will reduce the endurance of the drone.

The close-up nature of many aspects of the inspections of structures with drones means that the ability of the drones to navigate close to a structure and to hold a particular position near the structure for data collection is critical to prevent collisions with the structure. The ability of a drone to navigate and hold position precisely is negatively affected by wind. The capacity of a drone depends on the physical properties of the drone as well as the hardware and software it is utilizing; however, in one case, it was reported that a wind speed of 10 m/s (22 mph) made controlled flight near a structure nearly impossible [10]. Another study noted that high-quality imaging of a structure could not be captured with windspeeds greater than 7 m/s (16 mph) [6]. Some work has been done to develop open protective shells around drones for the close inspection of bridges [3]; however, such solutions likely increase drone weight and introduce drag which will collectively reduce the endurance of the drone. The challenges presented by wind are exacerbated by localized air flow patterns around structures, which result in areas of effectively higher winds and rougher air.

3.2 Data Processing Framework

In this research, a generalizable framework was developed for disaster relief efforts using drones. The methodological approach consists of two interrelated components: 1) processing drone-collected data, and 2) optimizing drone mission planning during disaster relief efforts. For data processing, 3D scene reconstruction and AI-based image processing can be integrated to help assess the situation, and extract disaster-relevant information for TDOT to make informed decisions. For 3D reconstruction, the SFM techniques are often employed. The SFM technique involves the below steps [9].

1. Features are detected for each of the images and metadata related to camera properties are extracted.
2. Features are matched across image pairs.
3. 3D reconstruction is initiated using an image pair with sufficient overlap and the associated camera properties of those images.

4. By using image features and an estimation of the camera pose, data from additional images are considered in the 3D reconstruction in an iterative process. The result of this is a sparse 3D point cloud.
5. The sparse 3D point cloud is then transformed into a dense 3D point cloud by using a pixel-wise image-matching algorithm to consider every pixel of the image set, not just features.

Commercial software such as Pix4Dmapper [52] and Agisoft [53] can also be used for 3D scene reconstruction. Figure 3-1 shows examples of 3D reconstruction for collapsed structures during Tennessee Tornado disasters and for bridge infrastructure systems.

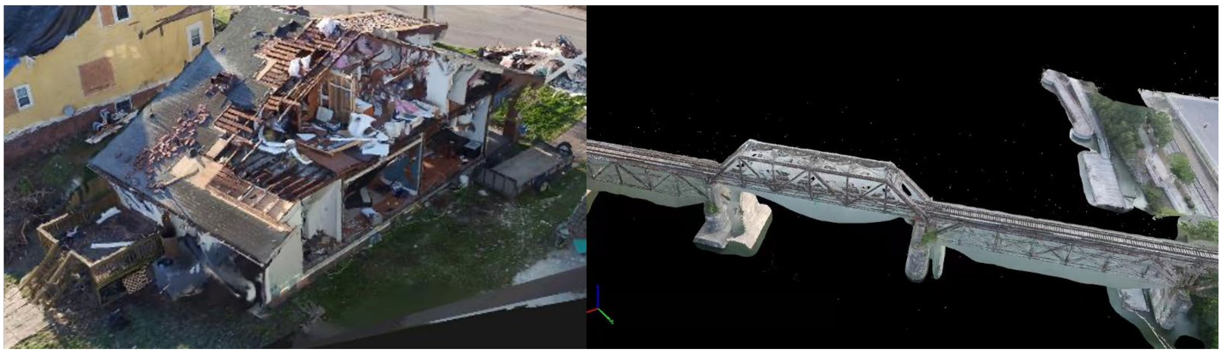

Figure 3-1 3D Reconstruction of Structures from Drone-Collected Images.

To recognize the object of interests (e.g., structure damages) from images captured by drones, a real-time deep learning-based network was designed. YOLO (You Only Look Once) was adapted in this study, which is a fast real-time multi-object detection algorithm [83]. Object detection in YOLO is done as a regression problem to estimate bounding box coordinates and class probabilities. CNN is employed to detect objects with a single forward propagation through the network, which can be trained in an end-to-end manner. The YOLOv5 network [84] used in this study is the latest upgrade from YOLOv3, adding mosaic, CSPNet, and SPPF module. YOLOv5 could be divided into YOLOv5-x6, l6, m6, and s6 based on the number of learnable parameters in the network. In this report, YOLOv5-l6 was selected to ensure the detection accuracy and inference speed. Figure 3-2 presents the YOLOv5-l6 network architecture that consists of three components that are backbone network, detection neck, as well as four detection heads. The input images were first preprocessed using the mosaic method, which is a data augmentation method to improve network performance on small objects. The backbone network was used to extract features at various levels from images. This network was built based on Cross Stage Partial Networks (CSPNet) and Spatial Pyramid Pooling Fast (SPPF) layer. The CSPNet was used to reduce the computation cost while maintaining the inference power of the network by CSPNet integrating the gradient changes into the feature map from beginning to end. Each CSPNet network consists of three convolutional layers. SPPF was used to extract fine and coarse information by simultaneously pooling on multiple kernel sizes (5, 9, 13). The SPPF is the last layer of the backbone.

The detection neck aims to get feature pyramids from the backbone network. The feature pyramid was used to identify objects in various sizes and scales. The detection neck consists of six CSPNet Blocks. The four feature maps with different scales were used to predict targets of various sizes. Finally, these feature maps were divided into grids, and each grid consists of three anchors to predict the bounding box for the object. Note that anchor sizes are generated by k-means clustering on the labeled bounding box dimensions. For each grid, the network estimated the bounding box coordinate offset and classification probability. With adequate training data with respect to the disaster scenes and objects, the framework can be used to train the model for rapid image processing. In this project, the framework was tested using data collected from the Tennessee tornado disasters and used it for detecting and assessing building collapse.

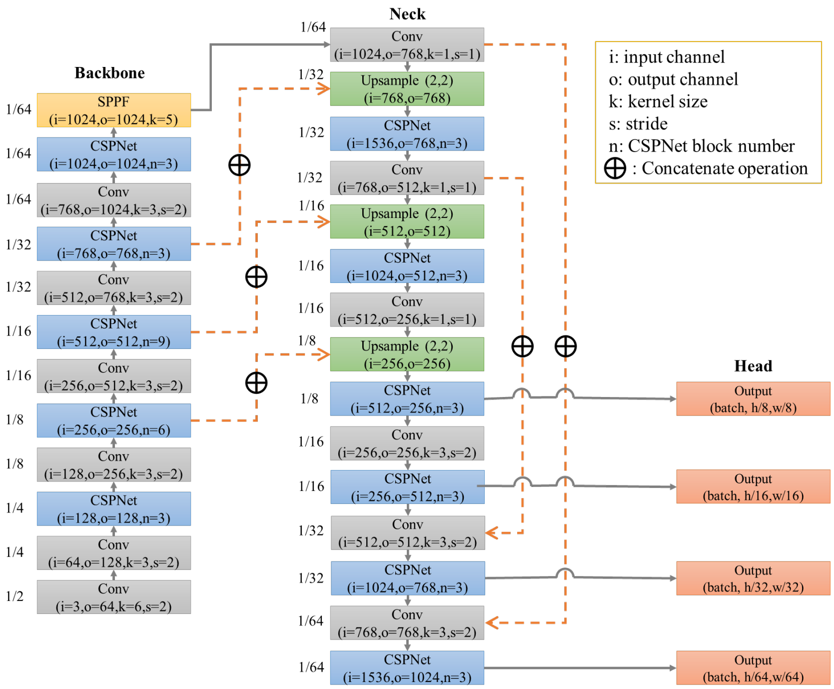

Figure 3-2 YOLOv5-l6 Network Architecture.

After recognizing the objects of interests (damage levels for different infrastructure systems), the drone needs to conduct a detailed investigation at each damaged site. The sequence of such investigation is related to the distance between damaged facilities and the drone, as well as the level of damages. This is because the extent of damage is an important indicator of property losses and investigation priorities. The drone needs to optimize the disaster survey plan according to detected damaged infrastructure with their associated severities to maximize the efficiency. To this end, the drone mission planning was formulated as a Vehicle Routing Problem with Profits (VRPP) [85]. The drone needs to survey a total of n damaged structures. Let $G = \{V, E\}$ be a graph. $V = \{1, \ldots, n\}$ is the vertices of the graph, which represent damaged structures. Each pair of vertices i and j forms an edge $\{i, j\} \in E$. Let the structure damage index $p_i \geq 0$ be associated with each vertex $i \in V$ (with $p_1 = 0$) and a distance $d_{ij} \geq 0$ be associated with each edge $(i, j) \in E$. Let x_{ij} be a binary variable which equals to 1 when the drone travel from i and j, and 0 otherwise. Let y_i equal to 1 if $i \in V$ is visited by the drone route, and 0 otherwise.

The objective was to maximize the total damage index visited by the drone given the traveled distance constraint. The damage index p_i is defined as 1, 3, and 5 for light, severe, and debris, respectively. The problem can be formulated in Eq. (3-1).

$$\text{maximize } \sum_{i \in V} p_i y_i \tag{3-1}$$

subject to

$$\sum_{j \in V\backslash\{i\}} x_{ij} = y_i \qquad i \in V, \tag{3-2}$$

$$\sum_{i \in V\backslash\{j\}} x_{ij} = y_j \qquad j \in V, \tag{3-3}$$

$$\sum_{i \in S} \sum_{j \in S\backslash\{i\}} x_{ij} \geq y_k \qquad S \subset V, i \in S, k \in V\backslash S, \tag{3-4}$$

$$\sum_{(i,j) \in E} d_{ij} x_{ij} \leq d_{max}, \tag{3-5}$$

$$\sum_{i \in V} p_i y_i \leq p_{min}, \tag{3-6}$$

$$y_i \in \{0,1\} \qquad i \in V, \tag{3-7}$$

$$x_{ij} \in \{0,1\} \qquad (i,j) \in E. \tag{3-8}$$

Constraints (3-2) and (3-3) are assignment constraints to ensure one edge enters and one edge leaves each visited vertex. Constraints (3-4) eliminate subtours. Constraint (3-5) is the maximum distance constraint on the route. Constraint (3-6) imposes to survey the structure with damage index not smaller than p_{min}. Finally, Constraints (3-7) and (3-8) are variable definitions.

Since the VRPP is NP-hard, the Tabu search (TS) [86] was adapted in this study to solve the problem. The TS is a metaheuristic algorithm that can be used for solving optimization problems. The method consists of 9 steps that are detailed as follows. The first step is to determine the tour length D and start building a tour until the length of route T reaches D. Vertex j was randomly selected in the tour T and add the vertex $j \notin T$ which has the minimal ratio $(d_{ij} + d_{jk} - d_{ik})/p_j$. The 2-opt optimization was applied on the generated list to delete two of the edges in the tour path and reconnect them in the remaining possible way. The second step determines all insertion partitions based on proximity measure and retains 10 of them. The dispersion index of the generated list R is given by Eq. (3-9).

$$\Gamma(R) = \begin{cases} \frac{1}{|R|(|R|-1)} \sum_{i,j \in R} d_{ij} & \text{if} |R|>1 \\ 0 & \text{if} |R|=1 \end{cases} \tag{3-9}$$

The proximity measure between to non-empty list R and S is defined in Eq. (3-10). Note that if $R=\{i\}$ and $S=\{j\}$, then $\Delta(R, S) = d_{ij}$. The proximity measure defines four partitions of $V \setminus \{1\}$, and each partition contains a cluster of vertices.

$$\Delta(R,S) = \frac{2}{|R||S|} \left(\sum_{i \in R, j \in R} d_{ij}\right) - \Gamma(R) - \Gamma(S) \tag{3-10}$$

The third step was used to determine the best insertion candidate from a randomly selected partition. The value of insertion of a cluster C'_{rk} from the partition Pr was calculated by dividing added damage index by distance. The gravity center $\bar{v}_k$ of C'_{rk} was computed for every cluster Pr. Eq. (3-11) can then be used to evaluate the preliminary move.

$$\bar{g}(C'_{sk}) = \frac{\sum_{v_h \in C'_{sk}} p_h}{l(T \cup \{\bar{v}_k\}) - l(T)} \quad (3\text{-}11)$$

The cluster C'_{sk^*} corresponding to $\max_k \{\bar{g}(C'_{sk})\}$ was selected. Eq. (3-12) gives the exact move evaluation for C'_{sk^*}.

$$\bar{g}(C'_{sk^*}) = \frac{\sum_{v_h \in C'_{sk^*}} p_h}{l(T \cup C'_{sk^*}) - l(T)} \quad (3\text{-}12)$$

The fourth step was used to determine the set of vertices H_{ij} candidate to be removed. Consider a solution $T = \{1, \dots, j_0, i_1, \dots, j_1, \ i_2, \dots, j_{k-1}, i_0, \dots, 1\}$, where (j_0, i_1), …, (j_{k-1}, i_0) have the longest edge in the route. The number of the longest edges was set to m, which was estimated between 2 and half of the maximum between 4 and the number of vertices in the initial tour. The sets H_{ij} were defined as $H_{i_1}, \dots, H_{i_{m-1} j_{m-1}}$.

The fifth step is used to determine the best deletion candidate from deletion chains, which is given in Eq. (3-13). The equation is associated with distance over lost damage index.

$$f(H_{ij}) = \frac{l(T) - l(T \setminus H_{ij})}{\sum_{v_k \in H_{ij}} p_k} \quad (3\text{-}13)$$

The sixth step compares the results of insertion and deletion and applies the best one. If the best move is deletion, then declare all vertices of deletion tabu for a random number of iterations. The seventh step applies 2-opt algorithm when the iteration count is a multiply of 5. The eighth step is used to improve the tour quality and make it an incumbent solution. The 3-opt algorithm was used to improve the newly generated solution when it has a better objective than the incumbent solution. Finally, if there hasn't been an improvement in 1000 iterations, the incumbent solution was assigned as the current solution and shuffle the route and clear the tabu list. The outcomes could help optimize drone mission planning, making the disaster reconnaissance more effective and efficient.

The proposed methodological framework could be adapted for application in different types of disasters and can be integrated with other commercial software and tools for acquiring important disaster relevant information for drone mission planning during disaster relief efforts.

Chapter 4 Results and Discussion

In Chapter 4, the use cases of using drones in different types of disaster scenarios and associated workflows are provided. The proposed methods were also tested using data collected from disasters such as tornado disaster occurred in the state of Tennessee and field demonstrations to validate the proposed methods and workflow. The use cases for post-disaster survey, landslide investigation, and flooding were discussed and insights for disaster preparedness, mitigation, response, and recovery are provided. Furthermore, the benefits and potential implementation for TDOT are also discussed herein.

4.1 Post-Disaster Infrastructure and Structure Survey

The use of drones for structural inspections has several key benefits compared to the traditional approach including 1) potential increases in the effectiveness and/or efficiency of the inspection and 2) increased safety of the inspection. Different methodologies and workflows for implementing drones for post-disaster infrastructure and structure surveys have been published including one by [8]. This methodology and its presentation provide a good example as it could be applied to many different structural assessments. A methodology, which is adapted from the methodology presented by [8], is represented by the flowchart shown in Figure 4-1 and is discussed in detail below.

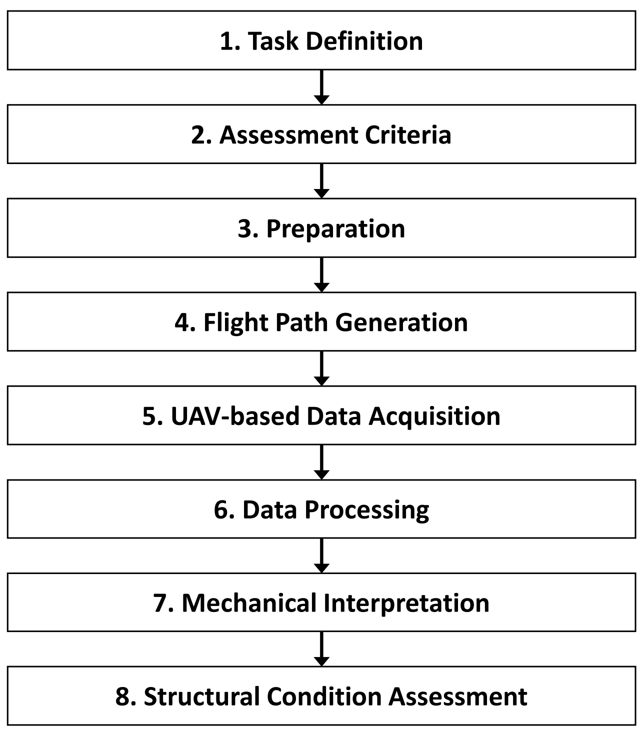

Figure 4-1 Flowchart for drone-assisted structural assessment (Adapted from [8]).

Step 1: Define the task to be undertaken and its purpose. This depends on the situation and may include tasks such as the overall assessment of the structure to comply with periodic inspection requirements, the assessment of particular members to determine the progression of deterioration at a trouble spot, or post-disaster assessment to determine if there is visible damage to the structure.

Step 2: Determine criteria to perform desired structural assessment. These criteria will depend on the structure being assessed, the types of members, and the construction materials. Potential criteria may include crack dimensions, spalled area percentages, rusted area percentage, and bearing deformation. When possible, numerical values should be established for the criteria that will determine structural condition; for example, the defined values of bearing deformation that would change the assessed condition of the structure.

Step 3: Prepare for the mission. In this step the points on the structure or portions of the structure in which data will be collected will be identified by considering construction plans, past assessments, and recent observations on the structure's state. The data types will be chosen for each data acquisition point to generate values to compare against the set assessment criteria. The necessary data types will aid in the selection of the drone and potential additional sensor package needed for the assessment. Obstacles that could impede a drone will be identified along with a point for launch and retrieval of the drone. This step could be aided by pre-inspection observations made by a drone, as described above.

Step 4: Generate the flight path. Regardless of if the drone will be piloted remotely or if its flight will be automated, a flight path must be established before flight. This flight path will move the drone from the launch point to and between the identified points of measurement and back to the launch point while avoiding hazards that have been identified. This flight path will also serve as a plan for the flight and should consider at each data collection point the sensors needed at that point, the orientation of the drone and the sensors at that point, and the time needed for the data collection at that point. The flight path should be as optimized as practical to minimize the total flight time required. The endurance of the drone must be conservatively accounted for in this flight plan and the flight should be broken up into multiple trips if needed. For automated flight, the results of the efforts of this step will be programed into the flight planning software utilized.

Step 5: Data is acquired with the drone. This data will be acquired based on the flight path.

Step 6: Once data is acquired, it needs to be processed. This processing will depend on the type of data that was acquired and the criteria that will be used to assess the structure. In many cases this data processing will use images, video, or other data to generate 3D representations of portions of the structure through photogrammetric techniques. After initial processing of the data, assessment criteria values will need to be extracted. This can be done in a manual manner or an automated manner depending on the criteria and the software available. For example, using SFM, images can be processed to create 3D representations of the state of a structural member; this 3D model can then be further processed using manual or automated techniques to identify and measure cracks.

Step 7: These results can then be used to provide a mechanical interpretation. Based on a collection of the features identified and potentially measured and the mechanics of the structure considered, a mechanical explanation for the behavior observed can be postulated. For example, the pattern of cracks observed may suggest the yielding of a component of the structure. In this step, structural analysis software could be used to investigate a potential mechanical interpretation and compare the predicted behavior with the behavior observed from the structure.

Step 8: A structural assessment can then be made. The assessment of the structure and components can be completed based on the processed data, any subsequent mechanical interpretation, the assessment criteria, the assessment task being performed, and any provided guidelines regarding the classifications resulting from the assessment.

The above structural assessment methodology can be implemented for planned structural assessments or in the event of the assessment of damage or potential damage to a structure from a disaster. The flight planning portion of this assessment requires significant resources and time; therefore, it may be advisable to generate and plan in advance for several general post-disaster structural assessment scenarios in order to be able to quickly respond to a disaster.

To test the proposed data processing framework for post-disaster structure survey and assessment, the designed network was first trained using the Instance Segmentation in Building Damage Assessment (ISBDA) [87]. The ISBDA dataset consists of a total of 1030 images extracted from ten aerial videos with a length of about 84 minutes collected from social media platforms. After removing images without bounding box annotation, the total number of images is 817. The videos were recorded using drones after severe hurricane and tornado disasters occurred in various states across the United States. The structure damage consists of three levels that are slight (visible cracks or appearance damage), severe (partial wall or roof collapse), and debris (completely structural collapse). Figure 4-2 presents example images with different damage levels.

Figure 4-2 Example of annotated images. The blue, green, and purple bound boxes denote damages in slight, severe, and debris levels, respectively.

The network was trained on a workstation running Windows 10 with Dual Intel Xeon Gold 5122 CPU, 64 GB RAM, and NVIDIA Quadro P5000. The Stochastic Gradient Descent (SGD) optimizer is used to train the network. The pretrained model on COCO dataset [88] was used to initialize network weights. The batch size was set to 48. The network was trained for a total of 30 epochs. The input images were resized to 640×640. The provided train-validation set was used for the training [87]. In total, the training set consists of 638 images, and the validation set consists of 219 images. The model with the highest performance on the validation set was used for further evaluation.

The hyperparameters of the model control various aspects of training, and it is challenging to find optimal values. YOLOv5-l6 contains a total of 29 hyperparameters, which are related to learning rate, loss function, data augmentation, etc. In this study, the hyperparameter evolution approach was used to find optimal values using the Genetic Algorithm (GA) optimization algorithm. The mutation-based genetic operator was used with a probability of 0.9 and a variance of 0.04. The epoch was set to 30 and the iterative was set to 100. Mean average precision over different IoU thresholds between 0.25 and 0.5 was used as the metric to determine the optimal parameters. Figure 4-3 shows example plots for some key optimized hyperparameters.

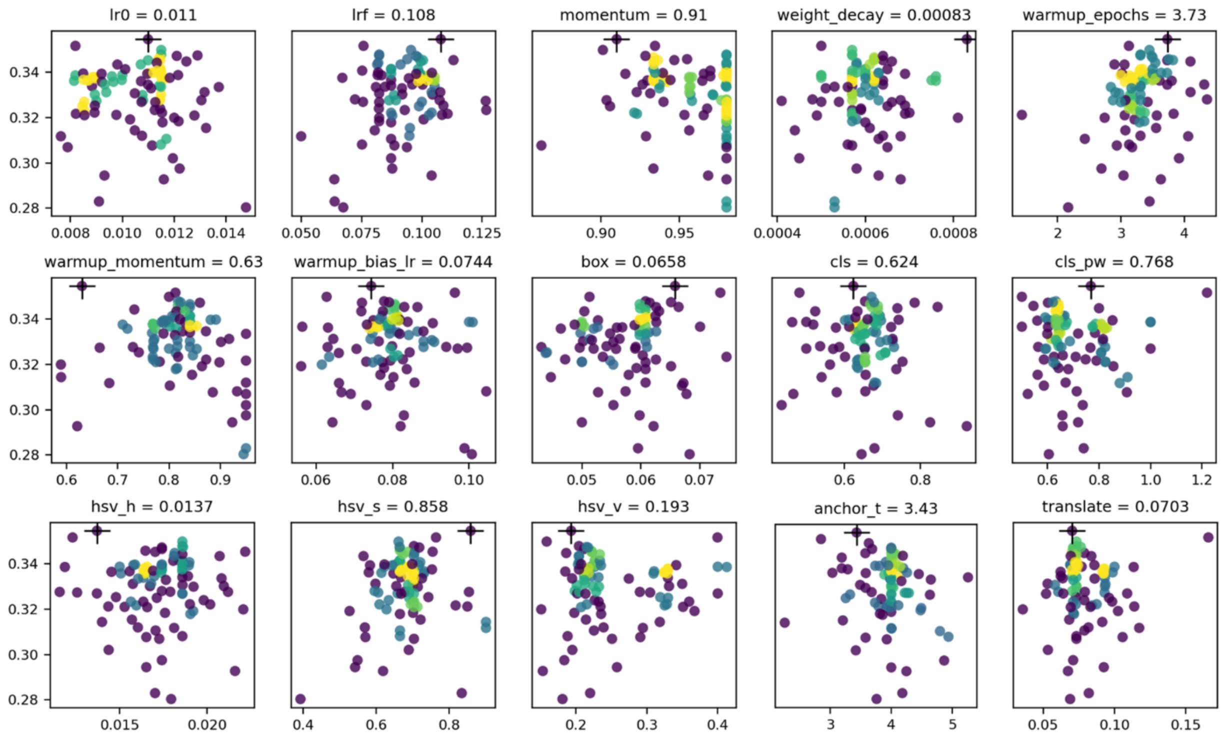

Figure 4-3 Optimized Hyperparameters for The Network Training.

To quantify the network performance, the recall, precision, mean average precision at IoU threshold 0.25 and 0.5 were used. Precision is used to measure the correctly classified positive against the total number of classified positives, which is defined in Eq. (4-1). Recall measures the predictive power of the network in identifying all the positive elements, which is given in Eq. (4-2). The IoU threshold is set to 0.2 for precision and recall calculations.

$$precision = \frac{1}{c}\sum_{i=1}^{c}\frac{TP_i}{TP_i+FP_i} \tag{4-1}$$

$$recall = \frac{1}{c}\sum_{i=1}^{c}\frac{TP_i}{TP_i+FN_i} \tag{4-2}$$

Following COCO setting, AP is the average over 10 IoU levels on the three damage categories. Average precision (AP) is the area under precision-recall curve that is defined in Eq. (4-3). *mAP* for object detection is the average of the AP calculated for all the classes, which is given in Eq. (4-4). $mAP_{0.25:0.5}$ is the average over 10 IoUs starting from 0.25 to 0.5 with a step size of 0.05.

$$AP = \int_{o}^{1}(\text{precision} \cdot \text{recall})\ d(\text{recall}) \tag{4-3}$$

$$mAP = \frac{1}{c}\sum_{i=1}^{c} AP_i \tag{4-4}$$

Furthermore, F1 score is used to set the inference confidence threshold for the evaluation, which is given in Eq. (4-5).

$$F1 = \frac{\text{precision}\cdot\text{recall}}{\text{precision}+\text{recall}} \tag{4-5}$$

Figure 4-4 shows the relationship between F1, precision, recall score and prediction confidence on the validation set of the ISBDA dataset. The results indicate that the highest F1 score is 0.43 at a confidence of 0.11. The precision score increases with an increasing confidence threshold value and the recall score decreases with the increasing threshold value. Furthermore, according to the recall score, light building damage has the highest ratio of correctly predicted positives to true positive elements at different thresholds.

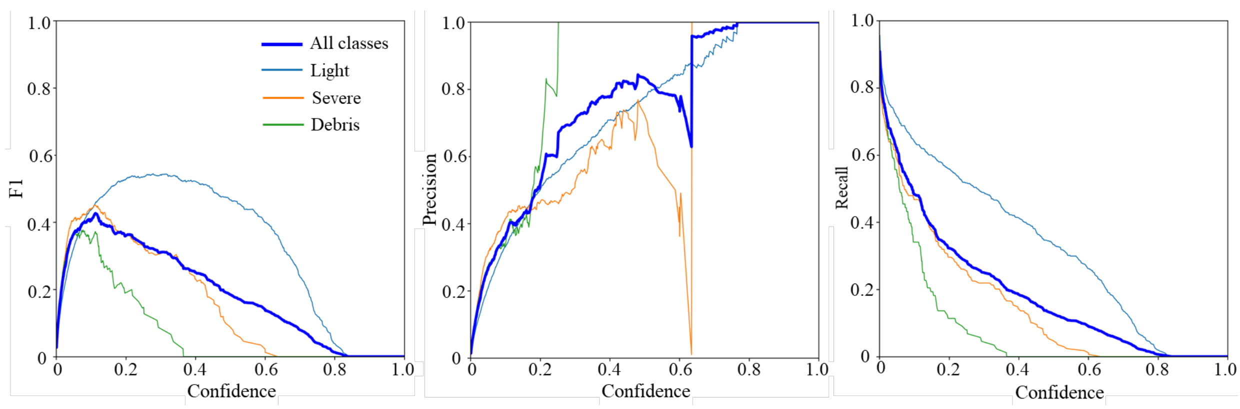

Figure 4-4 The Relationship Between F1, Precision, Recall Score and Prediction Confidence.

TABLE III presents the model performance on the validation set of the ISBDA dataset for each damage level. The overall precision, recall, $mAP_{0.25}$, $mAP_{0.5}$, and $mAP_{0.25:0.5}$ are 0.406, 0.473, 0.399, 0.289, and 0.345, respectively. The results of the proposed method indicate a strong variation in performance across different damage levels. Particularly, the proposed method results in the highest performance on the light building damage followed by severe damage. This is because the slight building damage has the largest amount of samples in the training dataset, and debris has a relatively small sample size.

TABLE III

DEEP LEARNING BASED STRUCTURE DAMAGE CLASSIFICATION FROM DRONE-COLLECTED DATA

Class	*Labels*	*Precision*	*Recall*	*$mAP_{0.25}$*	*$mAP_{0.5}$*	*$mAP_{0.25:0.5}$*
All	785	0.406	0.473	0.399	0.289	0.345
Light	528	0.391	0.621	0.52	0.347	0.427
Severe	169	0.425	0.491	0.361	0.265	0.314
Debris	88	0.402	0.307	0.318	0.256	0.293

Figure 4-5 illustrates four example results of damage detection in the validation set of the ISBDA dataset. The results indicate that the proposed method can accurately detect building damage and its associated level. The blue ellipses highlighted in the image show the damaged buildings that are not annotated in the dataset, but successfully detected by our network.

Figure 4-5 Visualization of Detected Damaged structures.

The research team also conducted a drone survey to collect aerial video data following tornado disasters in Tennessee. Figure 4-6 presents the example results of damage detection. The proposed method can detect structure damages from drone collected images, demonstrating its applicability and potential for disaster survey. Figure 4-7 shows the drone survey trajectory optimized using the proposed method. The center of the bounding box is treated as coordinates for the building. The drone needs to visit damaged structures to collect more information for further analysis. Figure 4-8 presents the optimized planning for the drone under different maximum distances constraints. The results indicate that the proposed mission planning method can identify the most efficient path for the drone to implement given a distance constraint.

Figure 4-6 Detected Building Damages from Post-Tornado Structure Surveys.

Figure 4-7 Drone Survey Trajectory and Overlaid Detected Damaged Buildings.

Figure 4-8 Optimized UAV Mission Plans for Different Distance Constraints.

The use cases and workflow for using drones to map subsurface infrastructures were also investigated. A 3D map of the ground needs to be created using a radio signal that can penetrate the scanned area [35,37]. This process first starts with flying an unmanned aerial vehicle (UAV) with a GPR module, TIR camera, or a flat speaker over the interest area. The reflected radio signals then need to be received in order by a GPR receiver, TIR camera, or an LDV scanner. Upon acquiring the reflected radio signals, a 3D map of the subsurface infrastructure can be reconstructed using processes such as SAR algorithms and surface vibration measurements. Figure 4-9 displays a flowchart of the process of mapping subsurface infrastructures using GPR techniques or sound-induced surface vibration systems. Various subsurface infrastructures exist underneath the roads in Tennessee that are aging and not all of them are properly mapped. The recommended practice by the report provides a fast and reliable method for TDOT and other agencies in the state of Tennessee to map the existing subsurface infrastructures and avoid causing unwanted damage to them by accidental excavations.

On the other hand, for inspecting subsurface infrastructure that has been mapped previously, TIR cameras deem to be the most powerful tool if the fluid carried within the buried pipeline has a heat gradient relative to the surrounding medium [31,33]. The inspection process begins with flying a TIR camera-mounted UAV over the subsurface infrastructure and acquiring TIR scans of the pipeline. The live-feed TIR scans can either be used to look for potential leakages or be saved to be post-processed and inspected to detect potential leakages. The TIR scans post-processing can be conducted using commercial software like FLIR Thermal Studio Suite [89]. Figure 4-10 shows the procedure for inspecting buried pipelines to detect potential leakages. The process suggested in this report provides a framework to identify any potential fluid leakage from the infrastructure systems underneath vital roads in the state of Tennessee. Implementing such a process not only provides an opportunity to inspect subsurface infrastructures following natural disasters in Tennessee but also can prevent disasters caused by high-pressured or flammable fluid leakages. In order to examine the proposed procedure for inspection of subsurface infrastructures, a demo flight was conducted on the University of Tennessee-Knoxville's steam lines. The thermal camera used in this flight was a FLIR Duo Pro R [90] with a resolution of 640 x 512 mounted on a DJI Matrice M600 Pro [38] equipped with a D-RTK system. The flight altitude varied between ~50 ft to 89 ft above the ground level (A.G.L.) depending on the terrain and the surrounding environment and obstacles. The acquired thermal images from the flight were analyzed using the FLIR Thermal Studio Suite. Figure 4-11 shows the thermal photo obtained from the steam line and the steam vault. Based on the acquired images the presence of the steam line has increased the surface temperature from about 28° C to ~32° C whereas the surface temperature directly above the steam vault has increased to ~38° C. In addition, locations of two potential leakages were identified using the TIR camera's live feed.

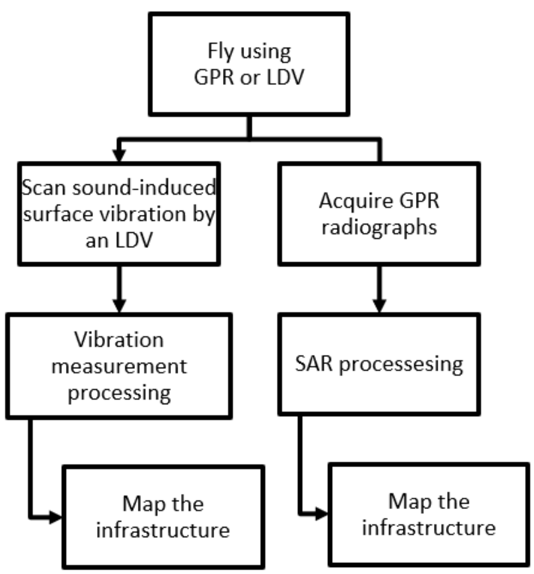

Figure 4-9 Flowchart for Mapping Subsurface Infrastructures.

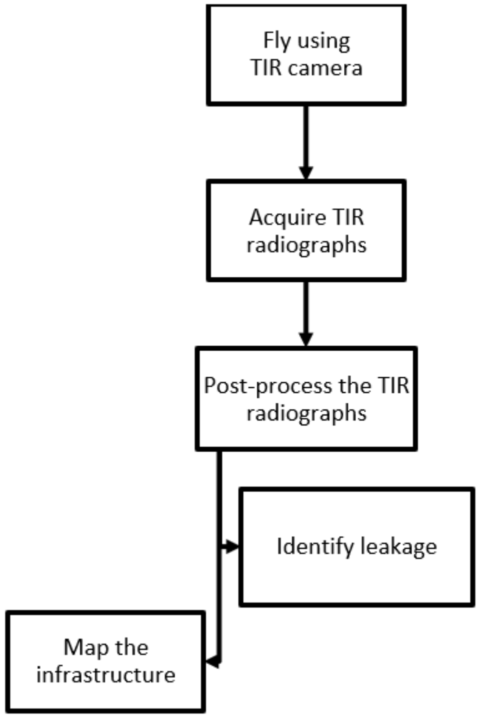

Figure 4-10 Flowchart for Identifying Potential Leaks from Subsurface Infrastructures.

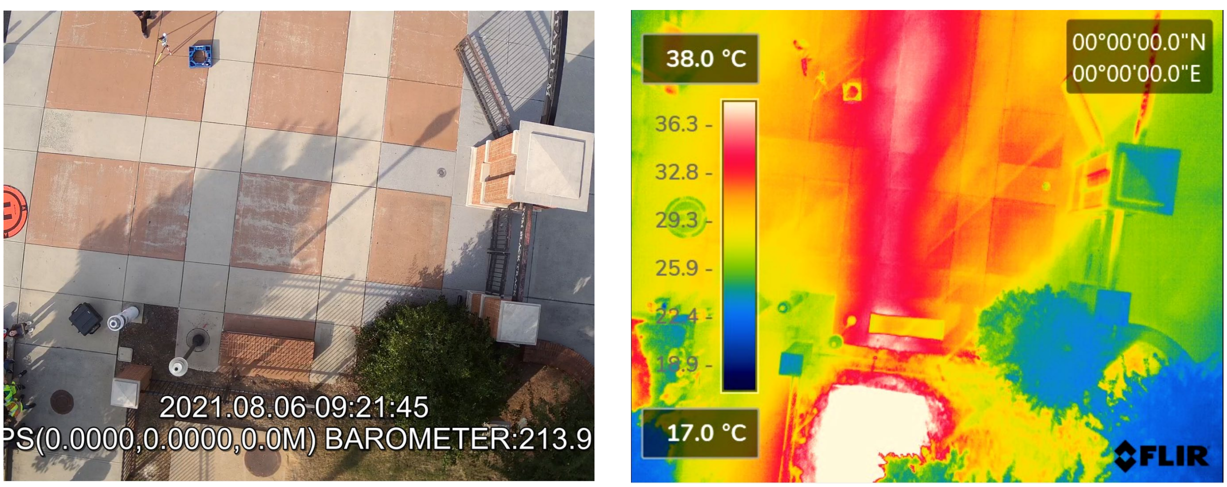

(a) RGB image **(b) Thermal image**

Figure 4-11 Aerial Image of The Steam Line and The Steam Vault.

Bridge pier scour inspections require mapping the stream bed around the piers of the bridge being inspected. The inspection can be performed by various types of underwater drones. Figure 4-12 shows a flowchart summarizing all needed hardware, software, and steps of bridge pier scour inspections. 19721 bridges exist in the state of Tennessee [91] and more bridges are being constructed each year in the state. Implementing a practice similar to the recommended practice by this report is a critical part of ensuring the safety of the existing bridges in the state.

An RTK-GPS module can be coupled into the underwater drone's GPS positioning system to improve the navigation and mapping results [92]. In addition, using a 2 MHz sonar sensor instead of a 1 MHz sonar sensor can further improve the mapping quality and accuracy [23]. Upon surveying the bridge piers, a map of the streambed can be reconstructed from the acquired sonar radiographs. The reconstructed map can be imported into CAD software to be viewed and search for potential scours around the bridge piers. Moreover, if an underwater drone is used in the inspection, the acquired images or even the live feed can be used to inspect the bridge piers for structural damages and cracks.

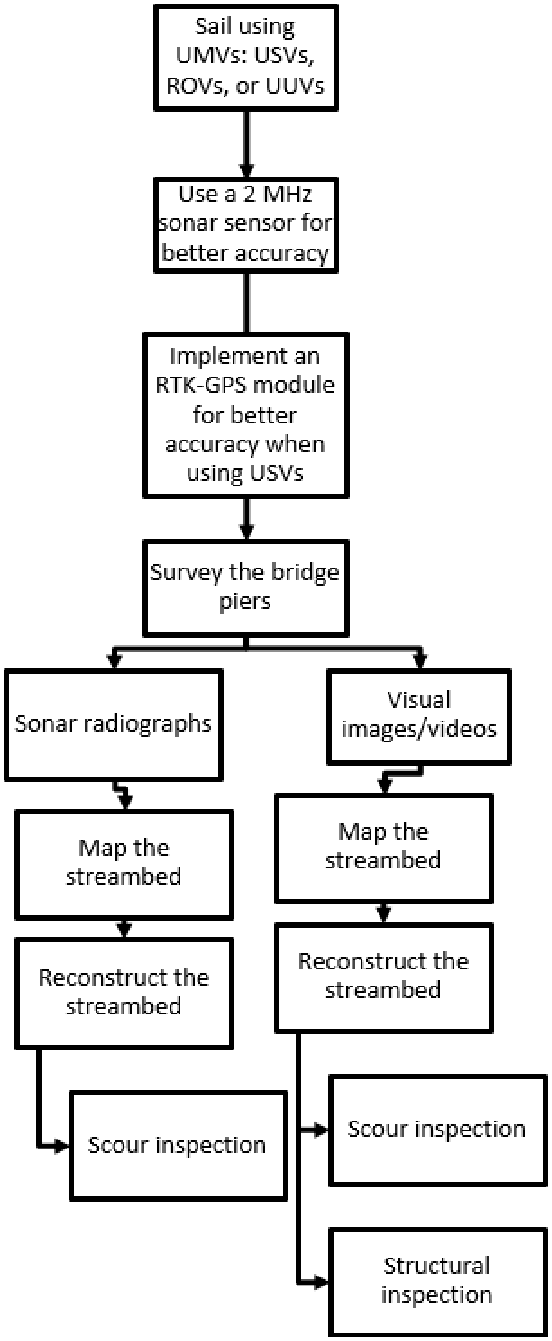

Figure 4-12 Flowchart for Bride Pier Scour and Structural Inspection.

4.2 Drone-Assisted Landslide Disaster Relief

The use cases and workflows for using drones in landslide disaster were also discussed herein. To identify a slope prone to landslides, a cloud point and an orthomosaic map of the slope need to be created. Information on primary factors causing landslides can then be overlaid on the generated map using GIS tools [47,50]. Pushpakumara & Madushanka [50] suggested the following factors as the primary causes of landslides: bedrock geology, hydrology & drainage, surface overburden, slope angle range, land use, and landforms, where these factors do not necessarily have equal probabilities of inducing a landslide (TABLE IV). A score can be assigned to each of the mentioned landslide factors based on the properties of the surveyed slope. A final probability score can be achieved by performing a weighted average on the 6 different scores assigned to the slope. The probability of a landslide can then be examined using TABLE V. Figure 4-13 shows the flowchart of the procedure to identify slopes with the potential for landslides. By implementing this practice TDOT or other agencies will be able to identify and rank the slopes that might experience landslides in the future. Regular monitoring procedures can then be set in place to ensure the safety of these slopes is not compromised.

TABLE IV

PRIMARY FACTORS CONTRIBUTING TO LANDSLIDES [50]

Slope		*Maximum Weighting*
1	Bedrock Geology	20
2	Hydrology & Drainage	20
3	Surface Overburden	10
4	Slope Angle range	25
5	Land use	15
6	Land forms	10
Total		100

TABLE V

PROBABILITY OF A LANDSLIDE [50]

Total Score	*Slope Failure Probability*
>70	Higher hazards
55-70	Medium hazards
40-55	Low hazards
40>	Not likely

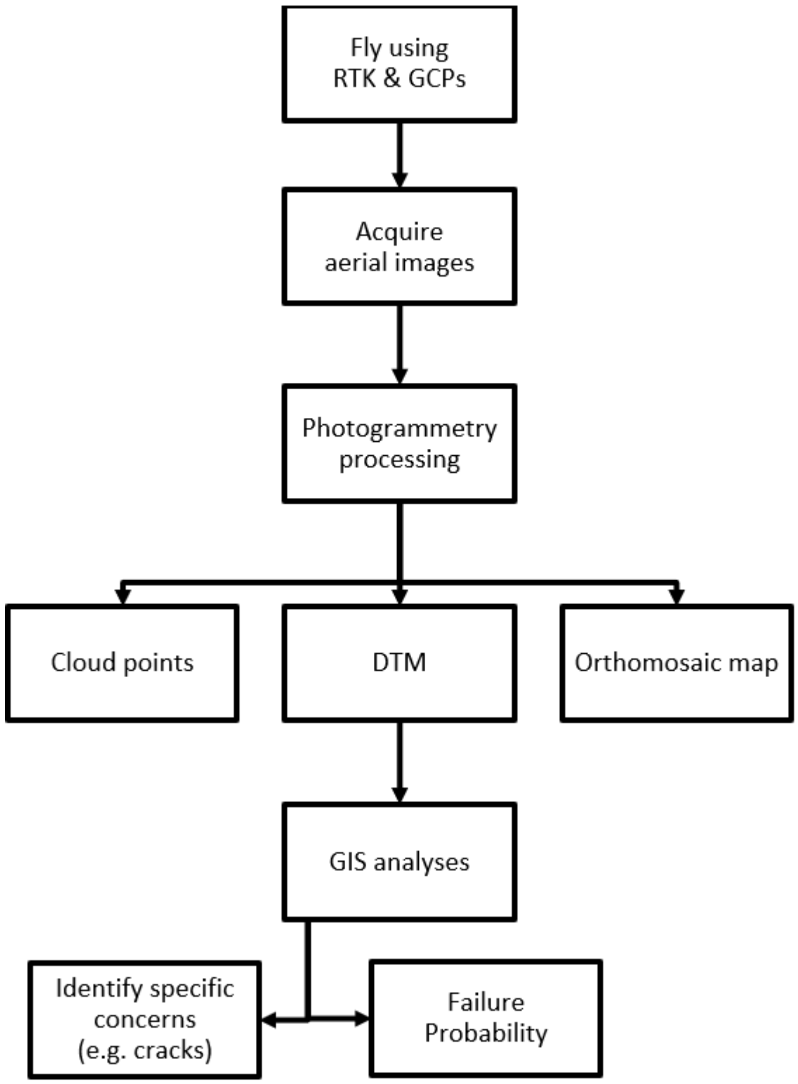

Figure 4-13 Flowchart for Identifying Slopes with Potential for Landslides.

Monitoring slopes with potential for landslides consists of using TIR/GPR/spectrometer sensors installed drones to estimate a slope's soil moisture content. First, a correlation between the results of any of the suggested sensors and soil moisture content needs to be established [48,55,56]. Regular drone flights can then be conducted on any slopes with the potential for landslides to determine the soil's moisture content. If the slope's moisture content exceeds the predetermined maximum safe moisture content, the slope either needs to be stabilized or evacuation measures need to be taken. The process of monitoring slopes prone to landslides can be summarized as the flowchart displayed in Figure 4-14. During each rain season, hundreds of small and large landslides occur in Tennessee, which most take place upon slope water saturation. Therefore, implementing the practice suggested in this report can help in preventing landslides and ensuring the safety of the drivers and roads in the state of Tennessee.

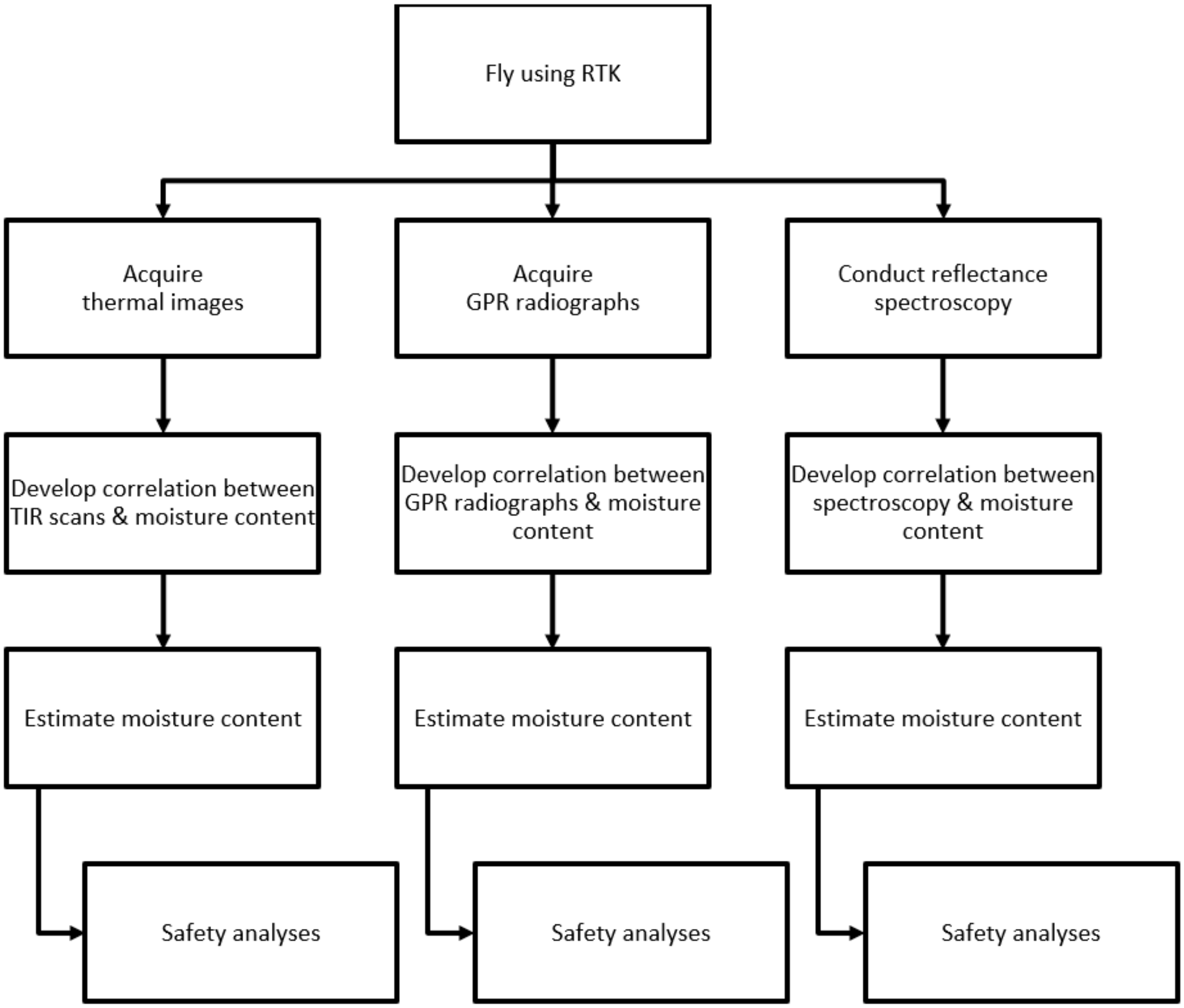

Figure 4-14 Flowchart for Monitoring Slopes with Potential for Landslides.

The first step in landslide disaster relief efforts is to map the affected area [59]. A relatively similar procedure to identifying the slopes with the potential for landslides can be performed to obtain a cloud point and an orthomosaic map of the slope. However, in this case, the results can be used to calculate the volume of the debris needed to be removed, design the new slope, and estimate the material required for reconstruction. Figure 4-15 shows the procedure of mapping a landslide using drones. As noted previously, hundreds of landslides (small or large) happen in Tennessee each year. First, a significant volume of debris must be moved post each landslide. The temporary shoring mechanisms and repair designs are then needed to open a road affected by the landslide to traffic. The recommended procedures here ensure the required steps for repairing a failed slope take place smoothly and in a timely manner.

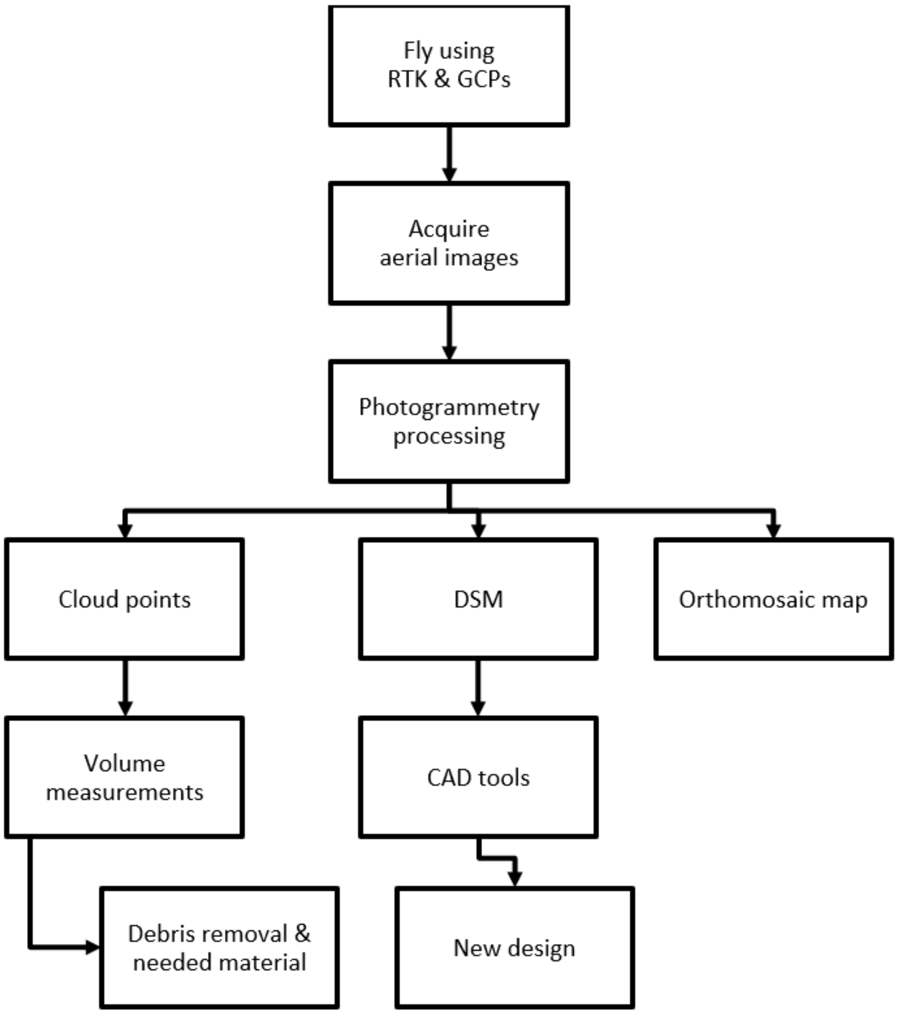

Figure 4-15 Flowchart for Mapping Landslide Post-Failure.

To examine the procedure of mapping a landslide, a complete topographic survey of a small shallow slope failure using a drone and employing photogrammetry was conducted by the research team. Figure 4-16 d shows an aerial image of the slope failure. In addition, to determine the dependency of the results on the flight height, flying at two different elevations was proposed. The selected flight elevations based on the site topography and obstacles were 196 and 262 ft A.G.L. . The flights were conducted using a DJI M210 RTK drone coupled with a Zenmuse X5s camera which is capable of capturing geo-located images with centimeter accuracy. Increasing the flight height from 196 ft A.G.L. to 262 A.G.L., which covered a considerably larger region of the slope, increased the total flight time from 2 minutes to 3 minutes and resulted in collecting 46 geo-located images instead of 16. Additionally, the accurate locations of 5 GCPs were collected (3 at the bottom of the slope and 2 at the top) using Propeller AeroPoints GPS receivers. Three of the GCPs were employed in the processing and calibration of the obtained geo-located images and the other 2 GCPs were used in the verification and determination of the survey accuracy. The obtained 2-dimensional geo-located images from the drone surveys were analyzed using the Pix4DMapper software. Figure 4-16 a, b, and c show the orthomosaic map, the DSM model, and the topographic map of the affected area, respectively. Comparing the accuracy of the 3D point cloud generated from the flights at different heights reveals that the accuracy of the coordinates of the generated points are extremely similar while the flight at the higher elevation covered a significantly larger area without increasing the flight time and processing time significantly.

(a) Affected area's orthomosaic map

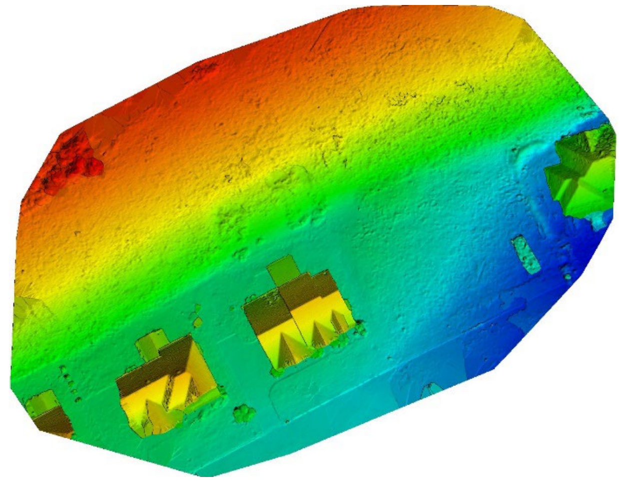

(b) Affected area's DSM model

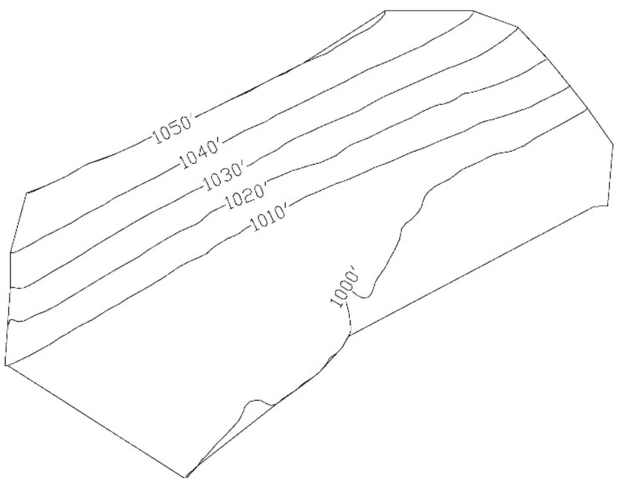

(c) Affected area's topographic map

(d) Aerial image of the slope failure

Figure 4-16 Demo Flight Results for Mapping a Small Shallow Landslide.

4.3 Drone-Assisted Flooding Disaster Relief

The first step in generating flood-risk assessment maps is to create a DTM of the area of interest. The process of creating DTM is identical to the process introduced earlier for surveying slopes prone to landslides. The area of interest's historical flood data is another necessary component of generating flood-risk assessment maps. The created DTM and the historical flood data can then be overlaid in GIS software such as ArcGIS [70] to generate flood-risk assessment maps [60,61,66,67]. Flood-risk assessment maps not only can be used to identify the areas that will be submerged during a flood but also can be employed for estimating the floodwater volume or the area of the flooded region. Figure 4-17 shows the flowchart for generating flood-risk assessment maps using UAV-based optical images. In cases water level gauges are used for increasing the accuracy of the river's stream depth, as recommended by Langhammer et al. [68], these additional data points can be treated as GCPs in the photogrammetry process. Flood-risk assessments are the initial step in designing and implementing measures for flood preparation. Implementing the suggested practices by this report help TDOT and other state agencies to identify the areas with high flooding risks and prepare the roads and other existing infrastructures accordingly.

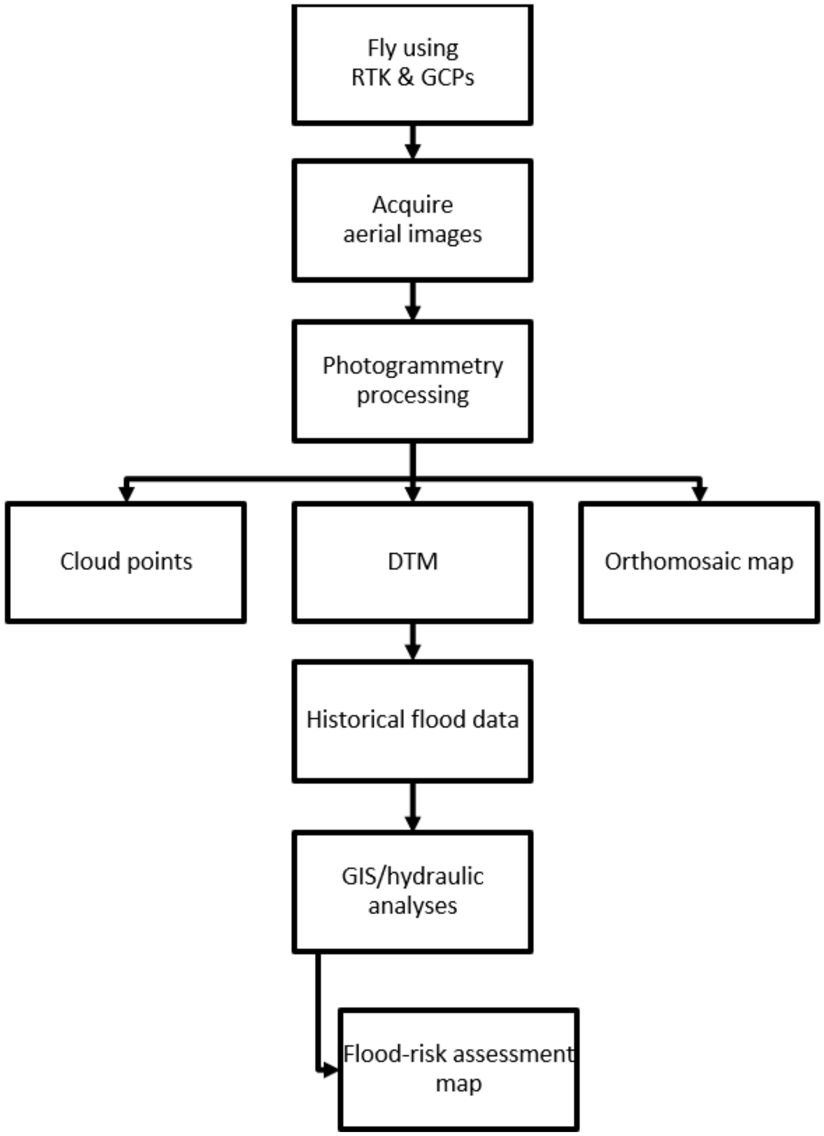

Figure 4-17 Flowchart for Flood-Risk Assessment Mapping.

Identifying the flooded areas during disaster relief efforts, start with flying over the area of interest and collecting optical images. The acquired images can be segmented into flooded areas and non-flooded areas using image processing techniques or a CNN [62,65]. The map created from the image processing techniques or neural networks identifies the extent of the flooded areas. Figure 4-18 shows the scheme of detecting flooded areas using a coupled CNN-RG method. The procedure recommended here provides the following opportunities to the state of Tennessee: identify the flooded areas following a flood for emergency disaster response efforts, determine the roads affected by the flood, and pinpoint the roads that are not flooded and may be used for disaster response efforts.

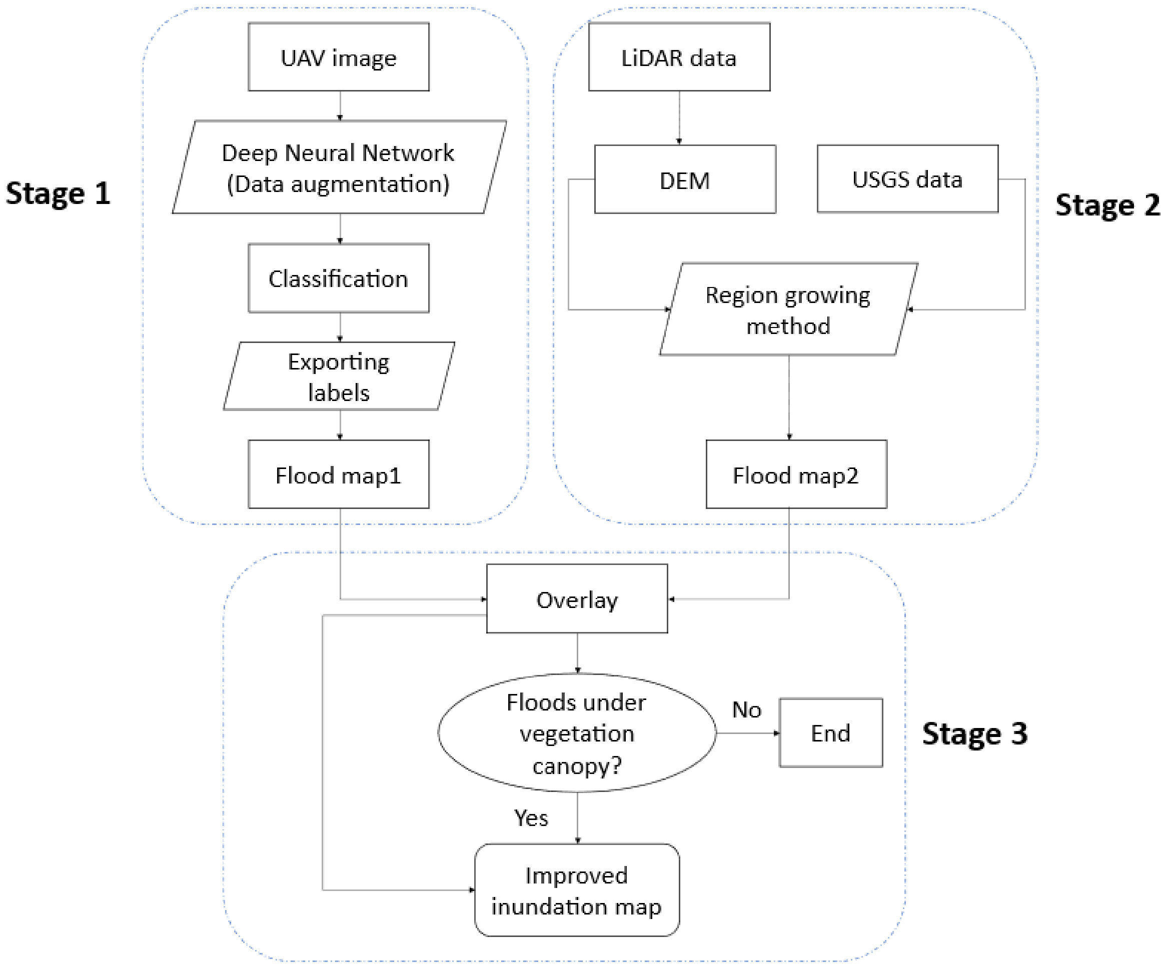

Figure 4-18 Flowchart for Detecting Flooded Areas (Adapted from [65]**).**

Post-floods, drone-based optical granulometry can be utilized for identifying the changes in granular materials affected by the flood, such as flood depositions. The optical granulometry method must be performed on optical images of the region of interest. Therefore, the first step in this process is to acquire aerial images of the affected area using an RTK drone system companied with GCP data points. An orthomosaic image of the affected area can then be created using photogrammetry processing on the acquired images. The orthomosaic image can be imported into an optical granulometry software such as BaseGrain [93] to identify the objects (grains) in the image. By obtaining the size of the grains identified in the image, the grain size distribution curves and parameters can be calculated. The generated grain size distribution data can then be compared with previously established grain size distribution data to detect the changes in the area's grain composition [68]. Figure 4-19 displays the flowchart for detecting grain size distribution changes post-floods using UAV-based optical granulometry. Many bridge abutment stabilizations in Tennessee use aggregates or riprap slopes. The mentioned aggregates might be displaced during a flood. The practice recommended by this study helps in detecting any changes in the bridge abutment aggregates after a flood to ensure the safety of bridges.

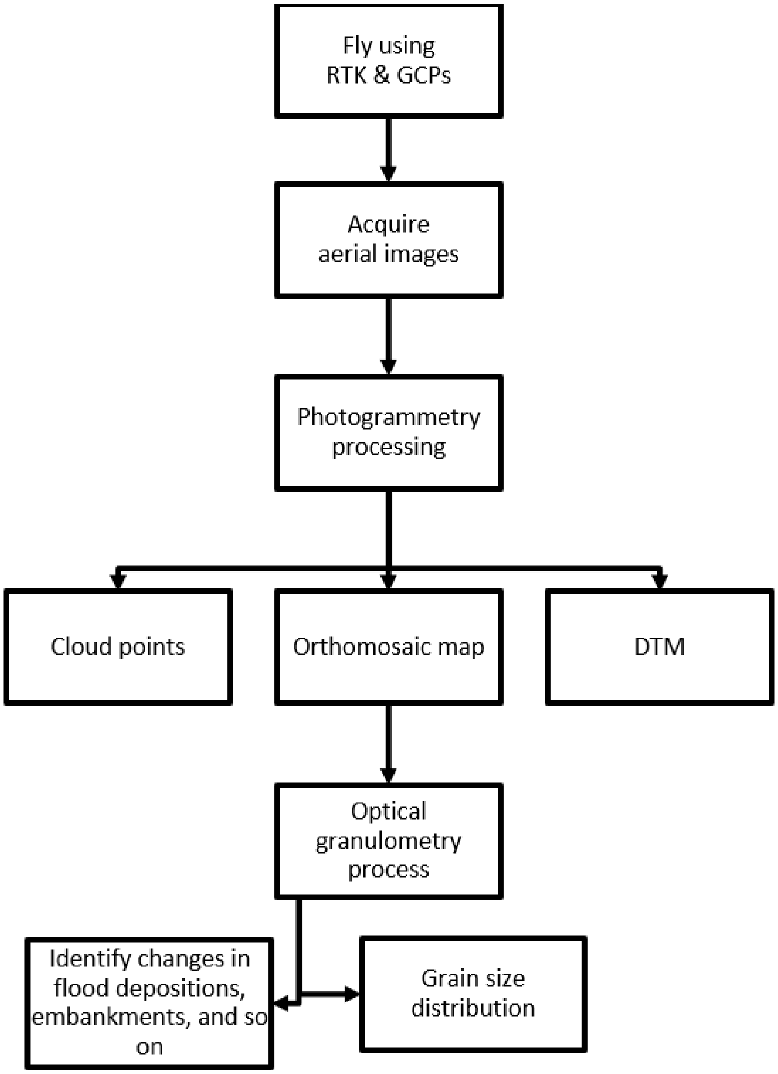

Figure 4-19 Flowchart for Optical Granulometry Using Drones.

4.3 Outcomes and Implementation Benefits

The outcomes from this project may yield potential benefits to TDOT for using drones during disaster relief efforts. First, this research led to a critical review of the hardware systems of drones and sensing technologies for application in different disaster relief efforts, sharpening TDOT's understanding about the capability and applicability of the emerging technologies. This outcome could expedite the usage of emerging technologies at TDOT and other state agencies to improve their technical capabilities in disaster relief. Drones have the potential to increase the effectiveness of disaster relief efforts such as infrastructure survey and assessment because their mobility gives drones the ability to inspect areas of a structure that are either inaccessible to inspectors or difficult / costly to reach. A key benefit of the use of drones for post-disaster assessments is that it can be used to reduce or eliminate many of the physical hazards faced by inspectors. These hazards include working at height, in isolated environments, in poor lighting conditions [1]. Even with proper training accidents do occur, so removing the interactions between hazards and inspectors is important. In addition to helping to preserve the health of inspectors, using drones to reduce the occurrence of injuries during post-disaster assessments can benefit the overall organization through less workman's compensation claims, less time away from work after injuries, and reduced liability [1]. In addition to reducing hazards for the inspectors during an assessment, the safety of inspectors can be improved by the drone providing information to assist in the planning of assessment activities. The use of drones to help facilitate post-disaster survey efforts are not necessarily limited to the actual inspection itself. Imaging from drones can be used to help in pre-inspection activities for disaster and structure assessments that will be later done with a detailed evaluation with drones or directly by traditional inspections. The data from drones in a pre-assessment can be used to identify areas where cleaning is required prior to assessment or areas where there is a particular concern of damage. Furthermore, this pre-inspection information can be used to plan a detailed path for the inspector or flight path for a UAV and identify hazards for the inspector (such as fall points, slips, sharp areas, vegetation, wildlife, etc.) or hazards for the drone (aerial obstructions, tight clearances, environmental concerns, etc.).

While drones have many benefits, their use has important constraints. The use of drones is not appropriate for all structures. For example, out of a randomly selected batch of bridges managed by the Oregon Department of Transportation, it was estimated that the inspection of 56% of these bridges would not benefit from drones [4]. One of the main reasons for this decreased set of bridges that would likely benefit from the use of drones was the assumption that small and short bridges could more easily be inspected by traditional means [4]. In another case, researchers found that the drone-based crack inspection took significantly longer than the average inspection time taken in 30 different hands-on inspections of the bridge they were examining [10]. Drones lack some basic capabilities that a physically present human inspector has. For example, the drone typically cannot be used perform hands on activities such as clear debris around a point that is desired for inspection or implement sounding-type tests. The mobility of drones is also compromised by difficulty or inability to operate in confined or interior spaces and their inability to clear obstacles such as closed doors or hatches. In addition to the physical constraints of drones, the Federal Aviation Administration rules that govern them place significant restrictions on their usage [94]. These restrictions include requiring visual line-of-sight operation, altitude limitations, weight limitations, certification requirements, and restrictions on operating over bystanders and vehicles.

Second, this research led to a generalizable framework for using drones and AI-enabled software/data processing tools, providing TDOT an implementable framework to process and analyze critical data before, during, and after disasters for disaster preparedness, response, and recovery. The framework was tested and validated using the data collected during the Tennessee tornado disasters, offering TDOT implementation insights for using the framework. The proposed framework entails two innovations: real-time structure damage detection and damage-aware drone mission planning, which collectively enable the drone to prioritize post-disaster efforts and acquire situational awareness regarding the affected disaster areas. It was also found that deep learning-based techniques are effective in detecting and classifying the region or objects of interests from the drone-collected images or videos. The detection network adopted in this research was trained on the ISBDA dataset and achieved an overall precision, recall, $mAP_{0.25}$, $mAP_{0.5}$, and $mAP_{0.25:0.5}$ of 0.406, 0.473, 0.399, 0.289, and 0.345, respectively, demonstrating its feasibility for practical applications in disaster relief efforts. For TDOT implementation, it should be noted that the results also indicate a strong variation in performance across different levels of structure damage. For instance, the light structure damage achieved the highest performance followed by the severe damage. Therefore, for practical application and interpretation, further evaluation and testing are still needed.

The feasibility of damage-aware UAV mission planning approach was also demonstrated in a experiment using the data collected after tornado disasters occurred in the state of Tennessee. The generated drone trajectory can maximize the total damage index given different distance constraints. The promising results show great potential for the proposed framework in improving the efficiency of disaster relief efforts using drones. For potential TDOT implementation, improvements in the following areas are needed. First, testing the proposed framework in real-world scenarios is needed to optimize the system based on the need for disaster relief operations. In addition, it is also necessary to evaluate to what extent the system will impact the efficiency of disaster relief efforts. Second, the structure damage detection accuracy is relatively low, which stems from the scarcity of training data. In the future, more data needs to be collected at disaster sites and advanced algorithms need to be developed. For other applications in disaster relief efforts, corresponding datasets also need to be prepared to train the deep learning-based techniques for practical implementation.

This research also produced uses cases and workflow for using drones in different types of disasters scenarios for potential implementation in Tennessee. The hardware systems for data acquisition, software systems for data processing, information management, and visualization were analyzed with respect to usage in different disaster scenarios. As such, TDOT could have a clear idea of what technologies and associated data analytics can be used in what scenarios and under what circumstances. The implementation of these advanced technologies could also help address several concerns that TDOT is facing with, including post-disaster surveys, landslide, and flooding. Therefore, this research could help TDOT to improve the efficiency and effectiveness of disaster preparedness, response, and recovery, and thus saving significant costs.

Chapter 5 Conclusion

Tennessee faces many threats from natural disasters such as tornadoes, flooding, landslides, and earthquakes, which damage civil infrastructure and cause major service interruptions. TDOT plays a critical role in preparing for, mitigating, responding to, and recovering from disasters. The use of advanced and emerging technologies such as drones, sensing technologies, machine learning methods, and optimization techniques could significantly expedite disaster relief efforts. Therefore, this research reviewed the current practice and system configurations for using drones and other emerging technologies in disaster relief efforts, providing useful insights for TDOT to understand the uses of these technologies. In addition, a generalizable framework based on 3D reconstruction, deep learning, and optimization was proposed for processing drone-acquired data and drone mission planning, which can be applied in various disaster scenarios. The framework can be adapted based on the needs from TDOT for potential implementation. This research also investigated the use cases as well as general workflows for using drone systems and software tools in different types of disaster scenarios, including post-disaster infrastructure systems surveys, landslide investigation, and flooding assessment. Pilot tests were also conducted to validate the proposed methods, use cases, and workflows, confirming the feasibility and potential of using drones and associated technologies in disaster relief efforts, and therefore providing TDOT useful information for potential implementation.

The key recommendations are summarized herein.

- First, with appropriate system configurations, drones can be used in various scenarios for disaster relief efforts to expedite the task implementation, improve data collection, and reduce survey and assessment time, as well as improve safety during disaster relief efforts. It should also be noted that different types of drones should be operated for different types of disaster scenarios, considering the constraints and limits of the drone systems, the requirement of disaster relief tasks, and the nature and environmental conditions of the disasters.
- Second, commercial software and tools are available to control drones and process drone-collected data for common applications such as 3D reconstruction. 3D reconstruction of disaster scene or structures of interest could provide useful models for subsequent analysis such as damage assessment and slope failure analysis. In addition, deep learning techniques can be applied to process drone-collected images for extracting disaster-relevant information with due accuracy. To achieve better performance, large amounts of training data are needed for more robust performance in disaster relief efforts.
- Third, the uses of drones in disaster relief efforts such as post-disaster infrastructure survey and assessment, landslide investigation, and flooding assessment are recommended. The workflows differ in different types of disasters and for different stages such as disaster preparedness, mitigation, response, and recovery, and practitioners need to carefully evaluate the workflow and use cases for practical applications

References

[1] D.W. Hubbard, The failure of risk management: Why it's broken and how to fix it, John Wiley & Sons, 2020.

[2] Mallela, Jagannath, Wheeler, Paul, Sankaran, Bharathwaj, Choi, Chan, Gensib, Elyssa, Tetreauat, Richard, Hardy, Darren, Integration of Unmanned Aircraft Systems into Operations Conducted by New England Departments of Transportation, 2021.

[3] C.J.O. Salaan, Y. Okada, S. Mizutani, T. Ishii, K. Koura, K. Ohno, S. Tadokoro, Close visual bridge inspection using a UAV with a passive rotating spherical shell, Journal of Field Robotics. 35 (2018) 850–867. https://doi.org/https://doi.org/10.1002/rob.21781.

[4] D.T. Gillins, C. Parrish, M.N. Gillins, C. Simpson, Eyes in the sky: Bridge inspections with unmanned aerial vehicles, 2018.

[5] J. Seo, L. Duque, J. Wacker, Drone-enabled bridge inspection methodology and application, Automation in Construction. 94 (2018) 112–126.

[6] D. Aldana-Rodríguez, D.L. Ávila-Granados, J.A. Villalba-Vidales, Use of unmanned aircraft systems for bridge inspection: a review, Dyna (Medellin). 88 (2021) 32–41.

[7] L. Otero-Cerdeira, F.J. Rodríguez-Martínez, A. Gómez-Rodríguez, Ontology matching: A literature review, Expert Systems with Applications. 42 (2015) 949–971.

[8] G. Morgenthal, N. Hallermann, J. Kersten, J. Taraben, P. Debus, M. Helmrich, V. Rodehorst, Framework for automated UAS-based structural condition assessment of bridges, Automation in Construction. 97 (2019) 77–95.

[9] A. Khaloo, D. Lattanzi, K. Cunningham, R. Dell'Andrea, M. Riley, Unmanned aerial vehicle inspection of the Placer River Trail Bridge through image-based 3D modelling, Structure and Infrastructure Engineering. 14 (2018) 124–136.

[10] S. Dorafshan, R.J. Thomas, M. Maguire, Comparison of deep convolutional neural networks and edge detectors for image-based crack detection in concrete, Construction and Building Materials. 186 (2018) 1031–1045.

[11] Y.-H. Chen, J.-T. Duh, S.-P. Huang, D.-H. Tsaur, J.-B. Ding, H.-J. Liao, Guidelines and procedures for post-earthquake safety evaluation and retrofitting of harbors and levees, Earthquake Engineering and Engineering Seismology. 3 (2001) 51–58.

[12] J. Choi, Y. Lee, T. Kim, J. Jung, H.-T. Choi, Development of a ROV for visual inspection of harbor structures, in: 2017 IEEE Underwater Technology (UT), IEEE, 2017: pp. 1–4.

[13] D.C. Jackson, N. Hundley Jr, William Mulholland and the St. Francis Dam disaster, California History. 82 (2004) 8–55.

[14] T. Ueda, H. Hirai, K. Fuchigami, R. Yuki, A. Jonghyun, S. Yasukawa, Y. Nishida, K. Ishii, T. Sonoda, K. Higashi, Inspection system for underwater structure of bridge pier, in: Proc. of International Conference on Artificial Life and Robotics, DOI, 2019.

[15] B.A. Bryan, Methods for assessing channel conditions related to scour-critical conditions at bridges in Tennessee, US Department of the Interior, US Geological Survey, 1995.

[16] P.F. Lagasse, E. v Richardson, ASCE compendium of stream stability and bridge scour papers, Journal of Hydraulic Engineering. 127 (2001) 531–533.

[17] P.L. Thompson, April 1989 Hatchie River US-51 bridge failure, Transportation Research Record. (1990).

[18] H. Hirai, K. Ishii, Development of Dam Inspection Underwater Robot., J. Robotics Netw. Artif. Life. 6 (2019) 18–22.

[19] J.E. DeVault, Robotic system for underwater inspection of bridge piers, IEEE Instrumentation & Measurement Magazine. 3 (2000) 32–37.

[20] R.R. Murphy, E. Steimle, M. Hall, M. Lindemuth, D. Trejo, S. Hurlebaus, Z. Medina-Cetina, D. Slocum, Robot-assisted bridge inspection, Journal of Intelligent & Robotic Systems. 64 (2011) 77–95.

[21] R. Pauly, C. Skrocki, Monitoring Scour Using Unmanned Vehicle Technology, Public Roads. 85 (2021).

[22] R.R. Murphy, E. Steimle, M. Hall, M. Lindemuth, D. Trejo, S. Hurlebaus, Z. Medina-Cetina, D. Slocum, Robot-assisted bridge inspection after Hurricane Ike, in: 2009 IEEE International Workshop on Safety, Security & Rescue Robotics (SSRR 2009), IEEE, 2009: pp. 1–5.

[23] C. Park, Y. Kim, H. Lee, S. Choi, H. Jung, Development of a 2 MHz sonar sensor for inspection of bridge substructures, Sensors. 18 (2018) 1222.

[24] S. Kim, E. Yoon, T.-C. Chien, H. Mustafa, P.H. Chou, M. Shinozuka, Smart wireless sensor system for lifeline health monitoring under a disaster event, in: Nondestructive Characterization for Composite Materials, Aerospace Engineering, Civil Infrastructure, and Homeland Security 2011, SPIE, 2011: pp. 694–706.

[25] N. Nojiima, Seismic vulnerability index for lifeline facilities, in: The 14th World Conference on Earthquake Engineering, China, 2008.

[26] S.E. Chang, Evaluating disaster mitigations: Methodology for urban infrastructure systems, Natural Hazards Review. 4 (2003) 186–196.

[27] G.P. Cimellaro, O. Villa, M. Bruneau, Resilience-based design of natural gas distribution networks, Journal of Infrastructure Systems. 21 (2015) 05014005.

[28] Y. Li, J. Gao, C. Jian, C. Ou, S. Hu, A two-stage post-disaster response and restoration method for the water distribution system, in: WDSA/CCWI Joint Conference Proceedings, 2018.

[29] L.J. Steinberg, A.M. Cruz, When natural and technological disasters collide: lessons from the Turkey earthquake of August 17, 1999, Natural Hazards Review. 5 (2004) 121–130.

[30] A. Braun, K. Parvar, M. Burns, UAV magnetometry in mineral exploration and infrastructure detection, in: AGU Fall Meeting Abstracts, 2015: pp. NH43C-1896.

[31] J. Kavi, U.B. Halabe, Detection of Buried Pipelines Transporting Hot Fluids using Infrared Thermography, (2020).

[32] M. Garcia-Fernandez, Y. Alvarez-Lopez, B. Gonzalez-Valdes, A. Arboleya-Arboleya, Y. Rodriguez-Vaqueiro, F. las Heras, A. Pino, UAV-mounted GPR for NDT applications, in: 2018 15th European Radar Conference (EuRAD), IEEE, 2018: pp. 2–5.

[33] S. Marathe, Leveraging drone based imaging technology for pipeline and RoU monitoring survey, in: SPE Symposium: Asia Pacific Health, Safety, Security, Environment and Social Responsibility, OnePetro, 2019.

[34] W.W. Greenwood, J.P. Lynch, D. Zekkos, Applications of UAVs in civil infrastructure, Journal of Infrastructure Systems. 25 (2019) 04019002.

[35] J. Colorado, M. Perez, I. Mondragon, D. Mendez, C. Parra, C. Devia, J. Martinez-Moritz, L. Neira, An integrated aerial system for landmine detection: SDR-based Ground Penetrating Radar onboard an autonomous drone, Advanced Robotics. 31 (2017) 791–808. https://doi.org/10.1080/01691864.2017.1351393.

[36] Y. Zhang, D. Orfeo, D. Burns, J. Miller, D. Huston, T. Xia, Buried nonmetallic object detection using bistatic ground penetrating radar with variable antenna elevation angle and height, in: Proc.SPIE, 2017. https://doi.org/10.1117/12.2260055.

[37] M. Garcia-Fernandez, Y. Alvarez-Lopez, F.L. Heras, B. Gonzalez-Valdes, Y. Rodriguez-Vaqueiro, A. Pino, A. Arboleya-Arboleya, GPR system onboard a UAV for non-invasive detection of buried objects, in: 2018 IEEE International Symposium on Antennas and Propagation & USNC/URSI National Radio Science Meeting, 2018: pp. 1967–1968. https://doi.org/10.1109/APUSNCURSINRSM.2018.8608907.

[38] DJI Matrice 600 Pro - DJI, (n.d.). https://www.dji.com/matrice600-pro (accessed April 1, 2022).

[39] T. Sugimoto, K. Sugimoto, I. Uechi, N. Utagawa, C. Kuroda, Fundamental Research on Shallow Underground Exploration Technology by Acoustic Irradiation Induced Vibration from UAV, in: 2020 IEEE International Ultrasonics Symposium (IUS), 2020: pp. 1–4. https://doi.org/10.1109/IUS46767.2020.9251573.

[40] Vibrometry products - PSV-500 Polytec Scanning Vibrometer - Polytec, (n.d.). https://www.polytec.com/us/vibrometry/products/full-field-vibrometers/psv-500-scanning-vibrometer (accessed April 1, 2022).

[41] B. Shakmak, A. Al-Habaibeh, Detection of water leakage in buried pipes using infrared technology; A comparative study of using high and low resolution infrared cameras for evaluating distant remote detection, in: 2015 IEEE Jordan Conference on Applied Electrical Engineering and Computing Technologies (AEECT), 2015: pp. 1–7. https://doi.org/10.1109/AEECT.2015.7360563.

[42] O. Hungr, S. Leroueil, L. Picarelli, The Varnes classification of landslide types, an update, Landslides. 11 (2014) 167–194.

[43] R.W. Jibson, D.K. Keefer, Landslides triggered by earthquakes in the central Mississippi Valley, Tennessee and Kentucky, (1988).

[44] R.W. Jibson, D.K. Keefer, Statistical analysis of factors affecting landslide distribution in the New Madrid seismic zone, Tennessee and Kentucky, Engineering Geology. 27 (1989) 509–542.

[45] R. Jowers, TDOT Counters Landslides Triggered by Floods of February, 2019, in: 70th Highway Geology SymposiumHighway Geology Symposium, 2019.

[46] S.K. Gupta, D.P. Shukla, Application of drone for landslide mapping, dimension estimation and its 3D reconstruction, Journal of the Indian Society of Remote Sensing. 46 (2018) 903–914.

[47] S.-W. Lin, T.-F. Hsueh, Using drone as a map to draw landslide hazard areas in the application of Community Environmental Education, in: IOP Conference Series: Earth and Environmental Science, IOP Publishing, 2019: p. 032057.

[48] R. Sobayo, H.-H. Wu, R. Ray, L. Qian, Integration of convolutional neural network and thermal images into soil moisture estimation, in: 2018 1st International Conference on Data Intelligence and Security (ICDIS), IEEE, 2018: pp. 207–210.

[49] P.D. Koutalakis, O.A. Tzoraki, G.I. Prazioutis, G.T. Gkiatas, G.N. Zaimes, Can drones map earth cracks? Landslide measurements in north greece using uav photogrammetry for nature-based solutions, Sustainability. 13 (2021) 4697.

[50] T.D.C. Pushpakumara, P. Madushanka, Analysis and Prediction of Landslide using Drone Image and GIS Techniques-Case Study Aranayaka Area, International Journal of Advanced Remote Sensing and GIS. 9 (2020) 3466–3472.

[51] Y. Taddia, F. Stecchi, A. Pellegrinelli, Using DJI Phantom 4 RTK drone for topographic mapping of coastal areas, The International Archives of Photogrammetry, Remote Sensing and Spatial Information Sciences. 42 (2019) 625–630.

[52] Discover PIX4Dmapper | Pix4D, (n.d.). https://www.pix4d.com/discover-pix4dmapper (accessed April 1, 2022).

[53] Agisoft Metashape, (n.d.). https://www.agisoft.com/ (accessed April 1, 2022).

[54] DJI Terra, (n.d.). https://www.dji.com/dji-terra (accessed April 1, 2022).

[55] K. Wu, G.A. Rodriguez, M. Zajc, E. Jacquemin, M. Clément, A. de Coster, S. Lambot, A new drone-borne GPR for soil moisture mapping, Remote Sensing of Environment. 235 (2019) 111456.

[56] J.S. Levy, J.T.E. Johnson, Remote soil moisture measurement from drone-borne reflectance spectroscopy: applications to hydroperiod measurement in desert playas, Remote Sensing. 13 (2021) 1035.

[57] S.G. Catane, N.A.S. Veracruz, J.R.R. Flora, C.M.M. Go, R.E. Enrera, E.R.U. Santos, Mechanism of a low-angle translational block slide: evidence from the September 2018 Naga landslide, Philippines, Landslides. 16 (2019) 1709–1719.

[58] C. Delacourt, P. Allemand, E. Berthier, D. Raucoules, B. Casson, P. Grandjean, C. Pambrun, E. Varel, Remote-sensing techniques for analysing landslide kinematics: a review, Bulletin de La Société Géologique de France. 178 (2007) 89–100.

[59] G. Rossi, L. Tanteri, V. Tofani, P. Vannocci, S. Moretti, N. Casagli, Multitemporal UAV surveys for landslide mapping and characterization, Landslides. 15 (2018) 1045–1052.

[60] A. Annis, F. Nardi, A. Petroselli, C. Apollonio, E. Arcangeletti, F. Tauro, C. Belli, R. Bianconi, S. Grimaldi, UAV-DEMs for small-scale flood hazard mapping, Water (Basel). 12 (2020) 1717.

[61] L. Hashemi-Beni, J. Jones, G. Thompson, C. Johnson, A. Gebrehiwot, Challenges and opportunities for UAV-based digital elevation model generation for flood-risk management: A case of princeville, north carolina, Sensors. 18 (2018) 3843.

[62] D. Popescu, L. Ichim, T. Caramihale, Flood areas detection based on UAV surveillance system, in: 2015 19th International Conference on System Theory, Control and Computing (ICSTCC), IEEE, 2015: pp. 753–758.

[63] P.R. Speer, C.R. Gamble, Magnitude and frequency of floods in the United States, US Government Printing Office, 1965.

[64] H. Yan, Magnitude and frequency of floods for rural, unregulated streams of Tennessee by L-Moments method, University of Arkansas, 2012.

[65] L. Hashemi-Beni, A.A. Gebrehiwot, Flood extent mapping: An integrated method using deep learning and region growing using UAV optical data, IEEE Journal of Selected Topics in Applied Earth Observations and Remote Sensing. 14 (2021) 2127–2135.

[66] J.R. Escobar Villanueva, L. Iglesias Martínez, J.I. Pérez Montiel, DEM generation from fixed-wing UAV imaging and LiDAR-derived ground control points for flood estimations, Sensors. 19 (2019) 3205.

[67] S. Coveney, K. Roberts, Lightweight UAV digital elevation models and orthoimagery for environmental applications: data accuracy evaluation and potential for river flood risk modelling, Int J Remote Sens. 38 (2017) 3159–3180.

[68] J. Langhammer, T. Lendzioch, J. Miřijovský, F. Hartvich, UAV-based optical granulometry as tool for detecting changes in structure of flood depositions, Remote Sensing. 9 (2017) 240.

[69] SenseFly, Swinglet CAM-user manual, Revision 2.2. (2011).

[70] 2D, 3D & 4D GIS Mapping Software | ArcGIS Pro, (n.d.). https://www.esri.com/en-us/arcgis/products/arcgis-pro/overview (accessed April 1, 2022).

[71] N. Casagli, W. Frodella, S. Morelli, V. Tofani, A. Ciampalini, E. Intrieri, F. Raspini, G. Rossi, L. Tanteri, P. Lu, Spaceborne, UAV and ground-based remote sensing techniques for landslide mapping, monitoring and early warning, Geoenvironmental Disasters. 4 (2017) 1–23.

[72] D. Chen, Z. Liu, L. Wang, M. Dou, J. Chen, H. Li, Natural disaster monitoring with wireless sensor networks: A case study of data-intensive applications upon low-cost scalable systems, Mobile Networks and Applications. 18 (2013) 651–663.

[73] J. Ueyama, H. Freitas, B.S. Faiçal, P.R. Geraldo Filho, P. Fini, G. Pessin, P.H. Gomes, L.A. Villas, Exploiting the use of unmanned aerial vehicles to provide resilience in wireless sensor networks, IEEE Communications Magazine. 52 (2014) 81–87.

[74] D. Popescu, L. Ichim, F. Stoican, Unmanned aerial vehicle systems for remote estimation of flooded areas based on complex image processing, Sensors. 17 (2017) 446.

[75] C. Kim, H. Moon, W. Lee, DATA MANAGEMENT FRAMEWORK OF DRONE-BASED 3D MODEL RECONSTRUCTION OF DISASTER SITE., International Archives of the Photogrammetry, Remote Sensing and Spatial Information Sciences. 4 (2016).

[76] K.-W. Chiang, G.-J. Tsai, Y.-H. Li, N. El-Sheimy, Development of LiDAR-based UAV system for environment reconstruction, IEEE Geoscience and Remote Sensing Letters. 14 (2017) 1790–1794.

[77] C.A. Baker, R.R. Rapp, E. Elwakil, J. Zhang, Infrastructure assessment post-disaster: Remotely sensing bridge structural damage by unmanned aerial vehicle in low-light conditions, Journal of Emergency Management. 18 (2020) 27–41.

[78] M. Rivas Casado, T. Irvine, S. Johnson, M. Palma, P. Leinster, The use of unmanned aerial vehicles to estimate direct tangible losses to residential properties from flood events: A case study of Cockermouth Following the Desmond Storm, Remote Sens (Basel). 10 (2018) 1548.

[79] C.C. Andrea, J.Q. Byron, P.I. Jorge, T.C.H. Inti, W.G. Aguilar, Geolocation and counting of people with aerial thermal imaging for rescue purposes, in: International Conference on Augmented Reality, Virtual Reality and Computer Graphics, Springer, 2018: pp. 171–182.

[80] M.I. Perdana, A. Risnumawan, I.A. Sulistijono, Automatic Aerial Victim Detection on Low-Cost Thermal Camera Using Convolutional Neural Network, in: 2020 International Symposium on Community-Centric Systems (CcS), IEEE, 2020: pp. 1–5.

[81] A. Maher, M. Inoue, Generating evacuation routes by using drone system and image analysis to track pedestrian and scan the area after disaster occurrence, in: Proceedings of the 10th SEATUC (South East Asian Technical University Consortium) Conference, Tokyo, Japan, 2016: pp. 22–24.

[82] D. Kang, Y. Cha, Autonomous UAVs for structural health monitoring using deep learning and an ultrasonic beacon system with geo-tagging, Computer-Aided Civil and Infrastructure Engineering. 33 (2018) 885–902.

[83] J. Redmon, S. Divvala, R. Girshick, A. Farhadi, You only look once: Unified, real-time object detection, in: Proceedings of the IEEE Conference on Computer Vision and Pattern Recognition, 2016: pp. 779–788.

[84] G. Jocher, A. Stoken, A. Chaurasia, J. Borovec, T. Xie, Y. Kwon, K. Michael, L. Changyu, J. Fang, V. Abrahim, Ultralytics/yolov5: v6. 0—YOLOv5n "Nano" Models, Roboflow Integration, Tensor, Flow Export, Open, CV DNN Support, Zenodo Tech. Rep. (2021).

[85] P. Vansteenwegen, W. Souffriau, D. van Oudheusden, The orienteering problem: A survey, European Journal of Operational Research. 209 (2011) 1–10.

[86] F. Glover, Tabu search—part I, ORSA Journal on Computing. 1 (1989) 190–206.

[87] X. Zhu, J. Liang, A. Hauptmann, Msnet: A multilevel instance segmentation network for natural disaster damage assessment in aerial videos, in: Proceedings of the IEEE/CVF Winter Conference on Applications of Computer Vision, 2021: pp. 2023–2032.

[88] T.-Y. Lin, M. Maire, S. Belongie, J. Hays, P. Perona, D. Ramanan, P. Dollár, C.L. Zitnick, Microsoft coco: Common objects in context, in: European Conference on Computer Vision, Springer, 2014: pp. 740–755.

[89] Teledyne FLIR, FLIR Thermal Studio Suite, (2021). https://www.flir.com/products/flir-thermal-studio-suite/.

[90] Teledyne FLIR, FLIR Duo® Pro R, (2021). https://www.flir.com/support/products/duo-pro-r/.

[91] 100 Years: Tennessee Bridges, (n.d.). https://www.tn.gov/tdot/100years-home/100years--bridges.html (accessed April 1, 2022).

[92] B. Matias, H. Oliveira, J. Almeida, A. Dias, H. Ferreira, A. Martins, E. Silva, High-accuracy low-cost RTK-GPS for an unmannned surface vehicle, in: OCEANS 2015-Genova, IEEE, 2015: pp. 1–4.

[93] M. Detert, V. Weitbrecht, User guide to gravelometric image analysis by BASEGRAIN, Advances in Science and Research. (2013) 1789–1795.

[94] C. Kamga, J. Sapphire, Y. Cui, B. Moghimidarzi, D. Khryashchev, Exploring Applications for Unmanned Aerial Systems (UAS) and Unmanned Ground Systems (UGS) in Enhanced Incident Management, Bridge Inspection, and Other Transportation Related Operations, (2017).